JCI The Journal of Clinical Investigation

Castration resistance in human prostate cancer is conferred by a frequently occurring androgen receptor splice variant

Shihua Sun, … , Peter S. Nelson, Stephen R. Plymate

J Clin Invest. 2010;120(8):2715-2730. https://doi.org/10.1172/JCI41824.

Research Article **Oncology**

Progression of prostate cancer following castration is associated with increased androgen receptor (AR) expression and signaling despite AR blockade. Recent studies suggest that these activities are due to the generation of constitutively active AR splice variants, but the mechanisms by which these splice variants could mediate such effects are not fully understood. Here we have identified what we believe to be a novel human AR splice variant in which exons 5, 6, and 7 are deleted (AR^{v567es}) and demonstrated that this variant can contribute to cancer progression in human prostate cancer xenograft models in mice following castration. We determined that, in human prostate cancer cell lines, AR^{v567es} functioned as a constitutively active receptor, increased expression of full-length AR (AR^{fl}), and enhanced the transcriptional activity of AR. In human xenografts, human prostate cancer cells transfected with AR^{v567es} cDNA formed tumors that were resistant to castration. Furthermore, the ratio of AR^{v567es} to AR^{fl} expression within the xenografts positively correlated with resistance to castration. Importantly, we also detected *AR^{v567es}* frequently in human prostate cancer metastases. In summary, these data indicate that constitutively active AR splice variants can contribute to the development of castration-resistant prostate cancers and may serve as biomarkers for patients who are likely to suffer from early recurrence and are candidates for therapies directly targeting the AR rather than ligand.

Castration resistance in human prostate cancer is conferred by a frequently occurring androgen receptor splice variant

Shihua Sun,[1] Cynthia C.T. Sprenger,[1] Robert L. Vessella,[2,3] Kathleen Haugk,[3] Kathryn Soriano,[1] Elahe A. Mostaghel,[1,4] Stephanie T. Page,[1] Ilsa M. Coleman,[4] Holly M. Nguyen,[2] Huiying Sun,[5] Peter S. Nelson,[1,2,4] and Stephen R. Plymate[1,2,3]

[1]Department of Medicine and [2]Department of Urology, University of Washington School of Medicine, Seattle, Washington, USA. [3]Geriatric Research, Education and Clinical Center, Veterans Affairs Puget Sound Health Care System, Seattle, Washington, USA. [4]Division of Human Biology, Fred Hutchinson Cancer Research Center, Seattle, Washington, USA. [5]Michael E. DeBakey Veterans Affairs Medical Center and Department of Medicine, Baylor College of Medicine, Houston, Texas, USA.

Progression of prostate cancer following castration is associated with increased androgen receptor (AR) expression and signaling despite AR blockade. Recent studies suggest that these activities are due to the generation of constitutively active AR splice variants, but the mechanisms by which these splice variants could mediate such effects are not fully understood. Here we have identified what we believe to be a novel human AR splice variant in which exons 5, 6, and 7 are deleted (AR^{v567es}) and demonstrated that this variant can contribute to cancer progression in human prostate cancer xenograft models in mice following castration. We determined that, in human prostate cancer cell lines, AR^{v567es} functioned as a constitutively active receptor, increased expression of full-length AR (AR^{fl}), and enhanced the transcriptional activity of AR. In human xenografts, human prostate cancer cells transfected with AR^{v567es} cDNA formed tumors that were resistant to castration. Furthermore, the ratio of AR^{v567es} to AR^{fl} expression within the xenografts positively correlated with resistance to castration. Importantly, we also detected *AR^{v567es}* frequently in human prostate cancer metastases. In summary, these data indicate that constitutively active AR splice variants can contribute to the development of castration-resistant prostate cancers and may serve as biomarkers for patients who are likely to suffer from early recurrence and are candidates for therapies directly targeting the AR rather than ligand.

Introduction

The androgen receptor (AR) is a principal driver of prostate cancer progression (1). This concept was first established by Huggins et al., with the demonstration that castration slowed, albeit temporarily, the progression of prostate cancer (2). Subsequent castration-resistant growth of prostate cancer has been attributed to a variety of mechanisms that include activation by receptor tyrosine kinases from growth factors, loss of cell cycle regulators, and rarely, genomic mutations in the AR allowing response to nonspecific AR ligands, such as progesterone or glucocorticoids (3–6). More recently, it was demonstrated that increased expression of the AR was the most common event associated with castration-resistant growth (7). Other studies support a process of metabolic adaptation, involving intracrine androgen synthesis (8–10). However, even when agents are used that decrease the tumoral androgen concentrations to very low levels, increased AR expression and signaling persists (11). In a percentage of tumors, the progression of prostate cancer is associated with activating AR mutations, but these events are infrequent (12). These observations suggest the possibility of alternative mechanisms, independent of androgenic ligands that maintain AR program activity in castration-resistant prostate cancers (CRPCs).

Recently, studies of cell lines and prostate cancers have identified several alternative splice forms of the AR (12–14). These AR variants have somewhat different structures, although each variant lacks portions of the ligand-binding domain (LBD), a feature predicted to produce a constitutively active receptor. Interestingly, the elevated expression of AR splice variants was found to be associated with more rapid disease recurrence following radical prostatectomy for localized disease, when compared with patients with lower expression of the variant (13, 15). Of additional interest, the splice forms were not expressed in the nucleus of normal prostate epithelium and rarely at substantial levels in primary prostate cancer. These data suggest that the presence of constitutively active splice variants of the AR arises following castration and plays a role in the progression of prostate cancer.

In this study, we report the identification and characterization of what we believe to be a previously unrecognized AR splice variant that comprises the full sequences of exons 1–4 and the full sequence of exon 8, skipping exons 5, 6, and 7 (hereafter referred to as AR^{v567es}, in which "v" denotes variant, and "es" denotes exons skipped). Because of the alternative splicing of exon 4 to the beginning of exon 8, a frame shift occurs that generates a new stop codon after the first 29 nucleotides of exon 8. Thus, the AR^{v567es} protein is not only smaller than the wild-type AR, but it terminates in a 10–amino acid sequence that we believe to be unique. We determined that AR^{v567es} is not only constitutively active but also increases expression of full-length AR (AR^{fl}) in the absence of ligand.

Results

Identification of AR variants in human prostate cancer xenografts. To identify alterations in the AR that could contribute to the

Authorship note: Shihua Sun and Cynthia C.T. Sprenger contributed equally to this work.

Conflict of interest: The authors have declared that no conflict of interest exists.

Citation for this article: *J Clin Invest.* 2010;120(8):2715–2730. doi:10.1172/JCI41824.

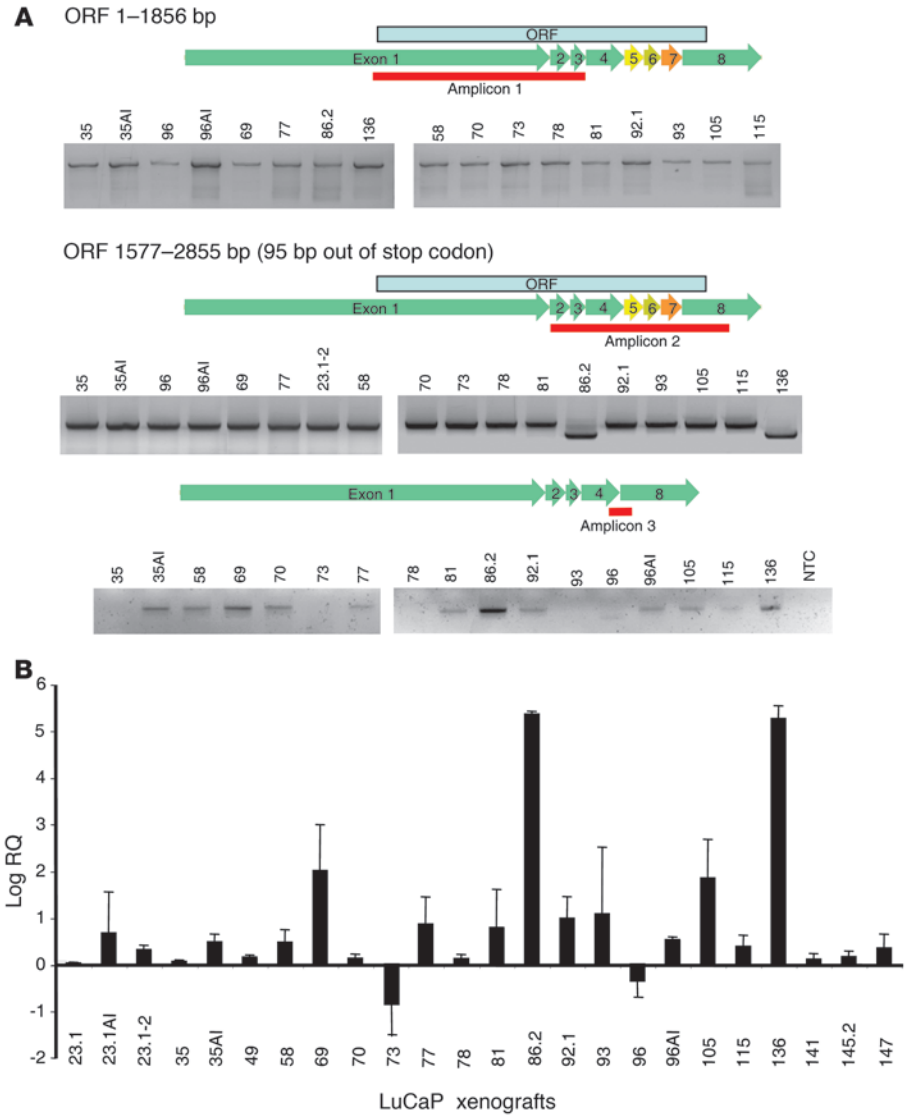

Figure 1
Identification of a novel AR splice variant. (**A**) Agarose gels showing PCR amplification of AR from human prostate LuCaP xenografts. Three sets of primers were used for PCR amplification of AR. One set is specific for exons 1–3 (amplicon 1), and another is specific for exons 2–8 (amplicon 2). The final set is specific for the 4–8 junction present in AR^{v567es} (amplicon 3). Note that xenografts 86.2 and 136 have a smaller PCR product with the amplicon 2 primers, while several xenografts are positive for the deletion using the amplicon 3 primers. Inverted agarose images are shown. NTC, no template control. (**B**) A graph of relative amounts of AR^{v567es} (amplicon 3) using qt-RT-PCR (mean ± 1 SD). Note that when xenografts occur as castrate-sensitive and castrate-resistant pairs (e.g., 35 and 35AI), the castrate-resistant sample (labeled AI) shows increased levels of AR^{v567es}. The differences were significant at $P < 0.05$ for 35 versus 35AI and 96 versus 96AI.

growth of CRPC, we used RT-PCR to measure AR transcript size in a panel of 25 different prostate cancer xenografts, termed the LuCaP series. Most of the LuCaP xenografts were derived from metastases obtained from men with CRPC, after prolonged exposure to androgen-deprivation therapy (ADT); however, their responses to castration, when grown in SCID mouse hosts, vary (Supplemental Table 1; supplemental material available online with this article; doi:10.1172/JCI41824DS1). We used 2 sets of primers to amplify exons 1–3 and exons 2–8 of the AR^{fl} cDNA (NCBI accession number NG_009014).

As shown in Figure 1A, 2 of the LuCaP xenografts, 86.2 and 136, express shorter AR transcripts in the region spanning exons 2–8, compared with AR^{fl} amplified in the remaining xenografts. We sequenced the short AR transcripts from LuCaP 86.2 and 136 and found identical cDNA sequences. In comparison to AR^{fl}, the variant *AR* mRNA from the LuCaP xenografts 86.2 and 136 lacks exons 5, 6, and 7, which encode the LBD of AR (AR^{v567es}; GenBank GU208210) (Figure 1A). While the full nucleotide sequence of exon 8 is present, due to the splicing of exon 4 to exon 8, a frame shift occurs in the ORF of AR^{v567es}. This frame shift results in a stop codon after the first 30 nucleotides, and thus, the amino acid sequence of exon 8 in AR^{v567es} is shortened to a 10–amino acid sequence, when compared with the amino acid sequence of exon 8 in the AR^{fl} (Supplemental Figure 1). The AR^{v567es} protein, therefore, is predicted to be 739 amino acids, compared with the 920–amino acid protein for AR^{fl}. The 2 xenografts, 86.2 and 136, were derived from 2 different patients who had undergone ADT during their clinical course. To address whether the AR^{v567es} variant was derived from a genomic mutation or alternative mRNA splicing, we extracted genomic DNA from the LuCaP 86.2 and 136 xenografts and determined the sequence of each AR exon and the intron flanking regions and found no differences when compared with the reference AR entry in GenBank (NM_000044). These results suggest that the AR^{v567es} variant transcript is a result of alternative mRNA splicing. We then designed primers to specifically detect the exon 4–8 junction present in AR^{v567es}, reexamined all the xenografts for the presence of the variant, and detected some level of variant AR in almost all xenograft samples (Figure 1, A and B). Interestingly, xenograft pairs comprising an androgen-sensitive derivative and a castration-resistant derivative expressed

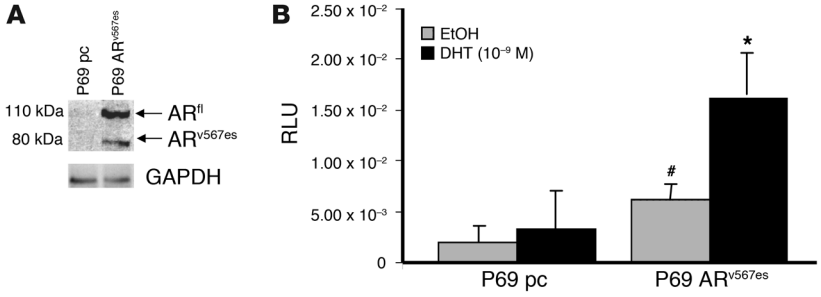

Figure 2

AR^{v567es} enhances AR^{fl} activity in benign prostate epithelial cells. (**A**) P69 SV40T immortalized, nontransformed human prostate epithelial cells transfected with AR^{v567es} demonstrated a marked increase in AR^{fl} protein compared with P69 pcDNA empty vector control cells (P69 pc). (**B**) ARR3-Luc reporter assay of P69 pcDNA control cells versus P69 AR^{v567es} cells, showing increased transcriptional activity basally and in response to DHT, consistent with increased AR^{fl} expression and AR^{v567es} expression (mean ± SEM). $^{\#}P < 0.05$, P69 AR^{v567es} compared with P69 pc control cells in the absence of androgen; $^{*}P < 0.01$, P69 AR^{v567es} compared with P69 pc cells with and without DHT added.

higher mRNA levels of *AR^{v567es}* in the castration-resistant sample (denoted by AI) compared with the androgen-sensitive sample (35 vs. 35AI and 96 vs. 96AI; $P < 0.05$).

The AR splice variant AR^{v567es} is constitutively active. To investigate the function of AR^{v567es} in both benign and cancer prostate cells, we cotransfected the P69 benign immortalized prostate epithelial cell line and the AR-null M12 human prostate cancer cell line, with the AR activity reporter construct pGL3-probasin ARE-ARR3-luciferase (ARR3-Luc) and a construct expressing AR^{v567es} (referred to as P69 AR^{v567es} cells and M12 AR^{v567es} cells, respectively). We also transfected the AR-null M12 cells with a wild-type AR^{fl} (referred to as M12 AR^{fl} cells). The pcDNA-AR^{v567es} expression vector expressed a protein of appropriate size for the AR^{v567es} cDNA in both benign and cancer cells (Figure 2A and Figure 3A). Interestingly, expression of AR^{v567es} in the benign P69 cells also resulted in expression of AR^{fl} (Figure 2A). Normally, AR^{fl} is only seen in these cells following dihydrotestosterone (DHT) treatment. Expression of the variant AR did not have this effect in the M12 cells (Figure 3A), which remained AR negative even after DHT treatment. As shown in Figure 2B and Figure 3B, expression of AR^{v567es} resulted in marked activity of the ARR3 reporter in the absence of the AR ligand DHT. The P69 AR^{v567es} cells, unlike the M12 AR^{v567es} cells, demonstrated a further enhancement in reporter activity following DHT treatment (Figure 2B and Figure 3B). The AR antagonist flutamide had no affect on the ARR3 reporter activity in M12 AR^{v567es} cells, whereas flutamide completely blocked DHT transactivation in the M12 AR^{fl} cells (Figure 3B). These data are consistent with a constitutively active AR^{v567es} without a functional LBD. In contrast, cells expressing an AR^{fl} required DHT to transactivate the ARR3 reporter construct.

To further evaluate the mechanism involved in constitutive AR^{v567es} activation, we stained the M12 cells transiently transfected with AR^{fl} or AR^{v567es} with an antibody specific to the N terminus of AR (sc441). In the absence of DHT, AR^{fl} was localized predominantly in the cytoplasm but translocated into the nucleus in the presence of DHT. In contrast, cells expressing AR^{v567es} consistently showed AR localized in the nucleus, regardless of the presence of DHT (Figure 3C).

Expression of AR^{v567es} in LNCaP cells increases the sensitivity of the endogenous AR to ligand. When AR^{v567es} was stably transfected into the AR^{fl}-positive LNCaP cells (LNCaP AR^{v567es} cells), we observed not only expression of the variant AR but also an increase in the amount of endogenous AR^{fl} protein compared with mock-transfected LNCaP cells (LNCaP pc cells) (Figure 4A and Figure 5A). This finding was consistent with observations in P69 cells engineered to express AR^{v567es} (Figure 2A). LNCaP AR^{v567es} cells grown in medium containing charcoal-stripped (CS) serum had the cuboidal appearance of control LNCaP pc cells grown in the presence of DHT (Figure 4B), whereas the control LNCaP pc cells grown in CS medium exhibited the expected elongated, stressed appearance of LNCaP cells grown without DHT. This alteration in morphology in the absence of DHT suggested that AR^{v567es} might function dominantly as a constitutively active AR in prostate cells that also express a AR^{fl}.

Following the introduction of the AR^{v567es} construct into LNCaP cells (referred to as LNCaP AR^{v567es} cells), an increase in basal ARR3 luciferase reporter activity was observed as well as a marked increase in reporter activity in response to DHT (Figure 4C), a finding that is concordant with the responses measured in P69 cells expressing AR^{v567es}. We then evaluated the DHT-induced changes in the expression of several androgen-induced genes (kallikrein-related peptidase 3 [*PSA*, also known as *KLK3*], transmembrane protease, serine 2 [*TMPRSS2*], FK506 binding protein 5 [*FKBP5*], NK3 homeobox 1 [*NKX3.1*], insulin-like growth factor 1 receptor [*IGF1R*]) using RT-PCR in the LNCaP pc cells versus the LNCaP AR^{v567es} cells (Figure 4D). The LNCaP AR^{v567es} cells had significantly higher mRNA levels for *PSA*, *TMPRSS2*, and *FKBP5* compared with those of LNCaP pc cells with and without DHT ($P < 0.001$ and $P < 0.0001$ compared with LNCaP pc cells with same treatment.). *NKX3.1* mRNA levels in the LNCaP AR^{v567es} cells were equally high, regardless of DHT exposure. Interestingly, *IGF1R* mRNA levels decreased in cells expressing AR^{v567es} compared LNCaP pc cells (Figure 4D), suggesting there is a functional difference between activation of AR^{fl} by ligand compared with the constitutively active AR^{v567es}. We expect that the difference in *IGF1R* mRNA levels is due to the fact that a nongenomic AR pathway regulates IGF-IR transcription; since AR^{v567es} primarily resides in the nucleus, the nongenomic pathway is not activated in these cells. Proliferation assays demonstrated that the LNCaP AR^{v567es} cells proliferated in response to lower concentrations of DHT than control LNCaP pc cells (Figure 4E). Together, these data suggest that the presence of AR^{v567es} enhances the transcriptional response of the endogenous AR^{fl} to androgens.

Because AR can autoregulate its own transcription and we saw an increase in AR^{fl} protein in the LNCaP AR^{v567es} cells, we wanted to determine whether the increased effect of the variant on androgen-regulated gene expression was simply through an increase in AR^{fl} protein levels. We overexpressed AR^{fl} in LNCaP cells and then performed ARR3-Luc reporter assays. Overexpression of AR^{fl} did result in increased AR^{fl} protein expression and increased reporter activity compared with that of LNCaP pc cells (Figure 5, A and B). But more importantly, even though LNCaP AR^{v567es} cells had a similar increase in AR^{fl} protein expression, they had significantly increased reporter activity compared with LNCaP AR^{fl} cells, indicating that the variant AR is affecting transcriptional activity to a greater degree than when AR^{fl} alone is amplified (Figure 5, A and B).

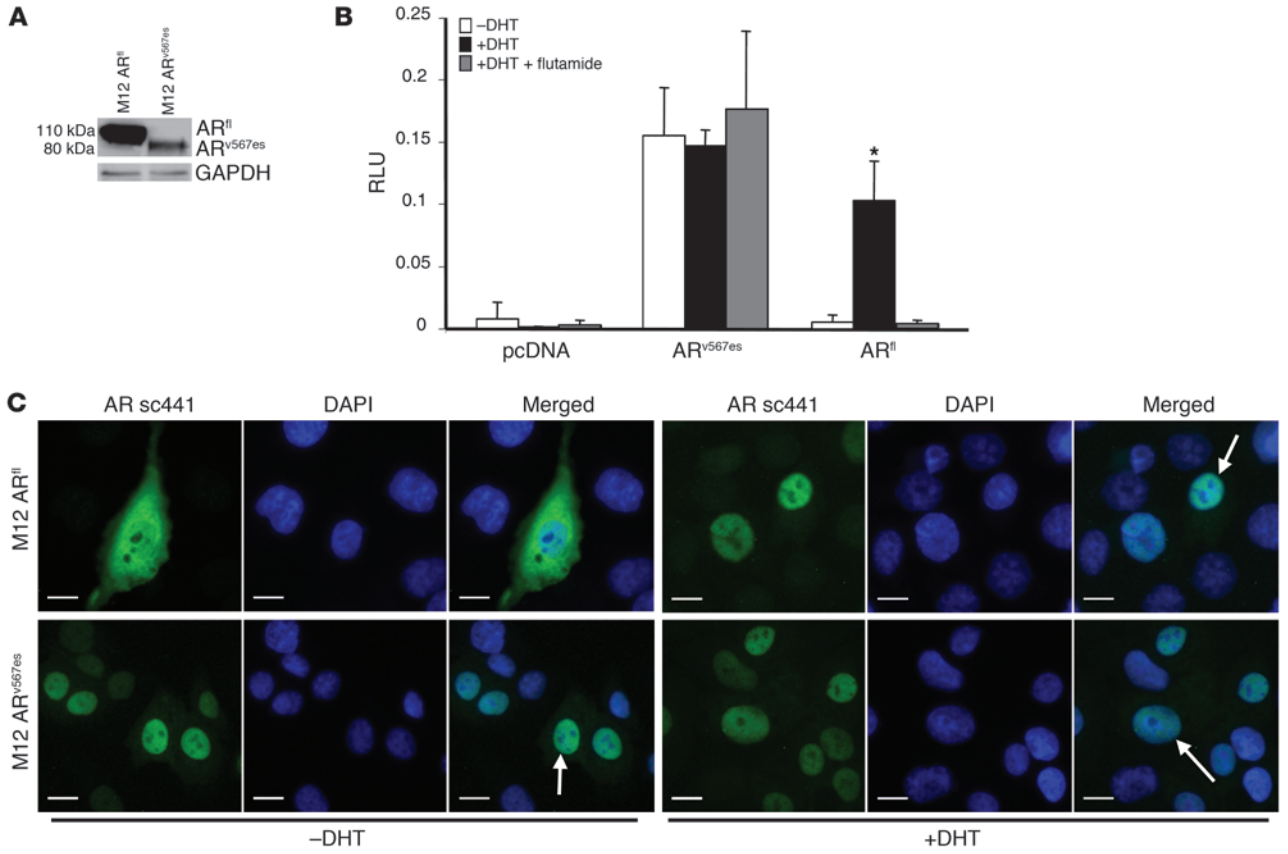

Figure 3

Constitutive activation of the AR^{v567es} in M12 prostate cancer cells. (**A**) The AR-null M12 human prostate cancer cells were transiently transfected with AR^{fl} or the splice variant AR^{v567es}. The Western immunoblot of transfected cells shows expression of either AR^{fl} or AR^{v567es}. AR was detected with AR sc441 antibody, which detects both full-length and variant AR. GAPDH was used as a loading control. (**B**) ARE luciferase assay with the ARR3-Luc reporter. The M12 pcDNA empty vector control cells show that no AR activity is detected for any of the treatments. The M12 AR^{fl} cells had very low reporter activity in the absence of androgen as well as in the presence of the AR antagonist, flutamide, but had a clear increase in luciferase activity when 10^{-9} M DHT was added. In contrast, M12 AR^{v567es} cells showed maximal reporter activity regardless of treatment. Values are mean ± SEM. *$P < 0.01$, DHT vs. no added DHT or DHT plus flutamide compared with DHT alone for AR^{fl}. There were no differences among treatments for pcDNA or AR^{v567es} cells. (**C**) Immunofluorescence staining of AR^{fl} and AR^{v567es}. In the absence of ligand, AR^{fl} is in the cytoplasm and translocates to the nucleus after addition of DHT. However, the constitutively active AR variant is primarily intranuclear in the absence of DHT and no change is seen when DHT is added. Nuclei are shown with DAPI staining. Arrows indicate examples of cells that are positive for nuclear translocation of AR. Scale bars: 10 μm.

AR^{v567es} binds to AR^{fl}. To further explore the mechanisms by which AR^{v567es} increases the activity of AR^{fl}, we expressed both AR^{fl} and a HA-tagged AR^{v567es} in the AR-null M12 cells and immunoprecipitated AR^{v567es} from cell lysates with an anti-HA antibody. Western blots were done on the immunoprecipitates using an N terminus–directed AR antibody (sc441), which recognizes both AR^{fl} and AR^{v567es}, and a C terminus AR–specific antibody (C-19), which recognizes only AR^{fl}, to detect any immunocomplex of the 2 ARs. As shown in Figure 6A, AR^{fl} coprecipitated with AR^{v567es} in the presence or absence of DHT, indicating a physical association of AR^{v567es} with AR^{fl}. M12 cells transfected with the empty pcDNA vector were used as a negative control, since these cells lack an endogenous AR. As a positive control, we cotransfected both an untagged and a Flag-tagged AR^{fl} into M12 cells, immunoprecipitated AR using a Flag antibody, and then immunoblotted with AR C-19 antibody (Figure 6A). In these cells, dimerization of AR^{fl} required ligand as opposed to the association of AR^{fl} and AR^{v567es} observed in the M12 AR^{fl} and AR^{v567es} cells in the absence of DHT. We then transfected M12 cells with either the AR^{fl} construct alone or both the AR^{fl} and AR^{v567es} constructs and performed immunofluorescence staining using the AR C-19 antibody, which detects only AR^{fl} protein. When both AR^{fl} and AR^{v567es} were present, AR^{fl} translocated to the nucleus in the absence of ligand, whereas it remained in the cytoplasm in cells expressing only AR^{fl} (Figure 6, B and C). To determine whether an interaction between AR^{fl} and AR^{v567es} occurs in tumors expressing both AR types, we immunoprecipitated AR^{fl} from lysates taken from castrate-resistant xenografts using the AR C-19 antibody and then immunoblotted them with AR sc441. We detected both full-length and variant AR in LuCaP 136 (strong AR^{v567es} band) and LuCaP 35 (weak AR^{v567es} band) xenografts (Figure 6D). These results suggest that in cells that endogenously express AR splice forms, the AR^{v567es} can functionally interact with AR^{fl}.

AR^{v567es} increases the stability of AR^{fl} protein. Because we observed an increase in AR^{fl} protein levels without a long-term increase in *AR^{fl}* mRNA levels (Figure 7A) and there appeared to be an interac-

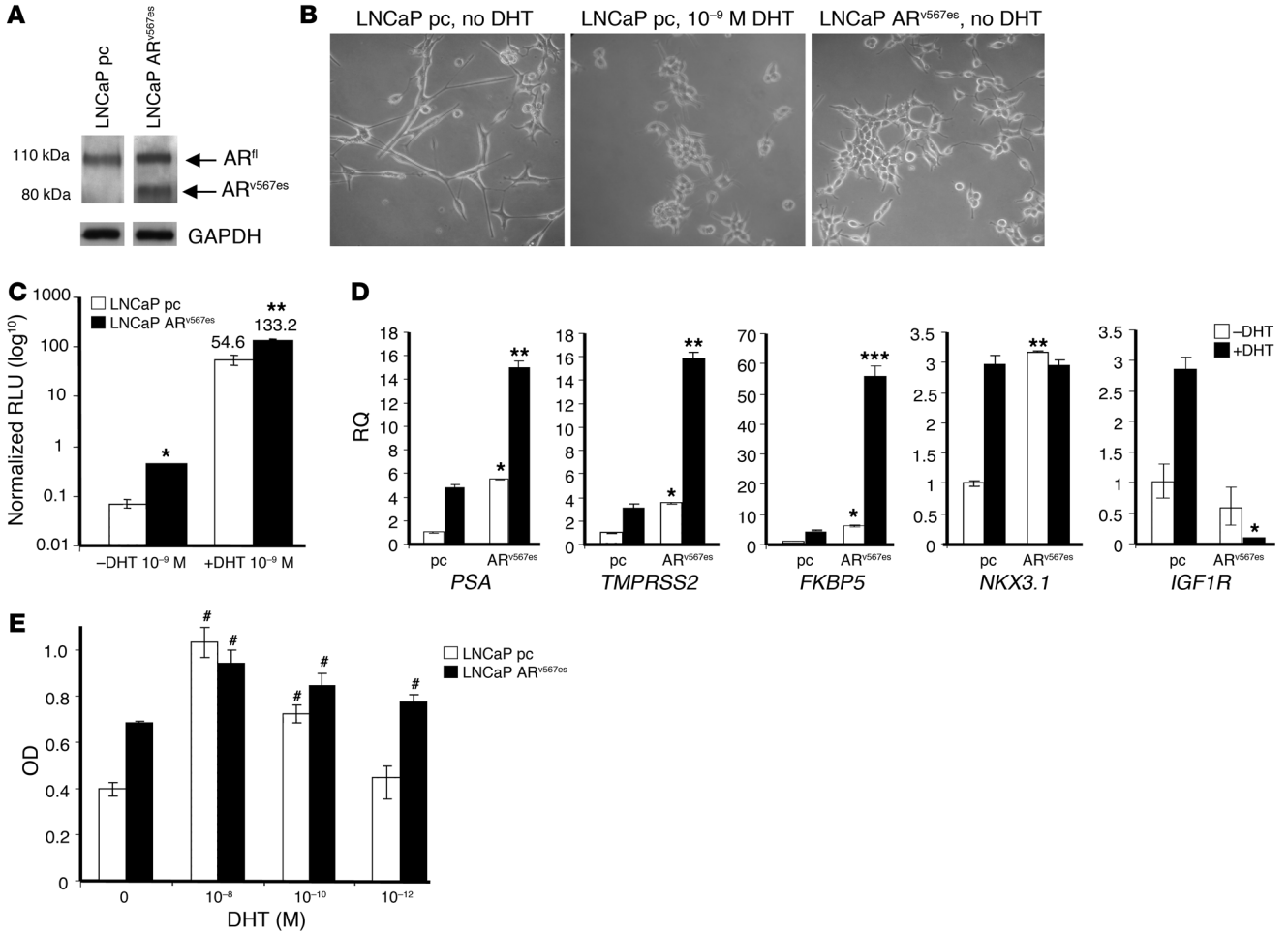

Figure 4

Increased AR^{fl} activity in LNCaP cells transfected with AR^{v567es}. The AR-positive LNCaP cells were transfected with AR^{v567es} or empty vector (pcDNA). (**A**) Western blot using AR sc441 antibody, which detects both AR^{fl} and AR^{v567es}. In cells transfected with AR^{v567es}, the AR^{fl} protein is markedly increased over that of control cells. Lanes were run on the same gel but were noncontiguous. (**B**) LNCaP cells were grown in vitro in CS serum. Cells containing the constituently active AR^{v567es} had the cuboidal appearance of the androgen-treated LNCaP cells. Original magnification, ×100. (**C**) Luciferase ARR3-Luc reporter assays performed on LNCaP cells showed a significant increase in AR signaling in the absence of DHT for cells expressing the AR^{v567es} protein. When DHT was added, there was a further increase in AR transactivation in the AR^{v567es} cells (133.2 RLU) compared with LNCaP pc control cells (54.6 RLU). *$P < 0.01$, **$P < 0.001$. (**D**) mRNA from several AR-regulated genes was examined by qt-RT-PCR (RQ). Interestingly, IGF-IR, which is regulated by nongenomic activities of the AR, was suppressed by the presence of AR^{v567es}, suggesting a loss of nongenomic AR activity by the variant. *$P < 0.01$, **$P < 0.001$, ***$P < 0.0001$, compared with LNCaP pc cells with same treatment. (**E**) MTS assay of LNCaP pc and LNCaP AR^{v567es} cells treated with decreasing concentrations of DHT. $^{\#}P < 0.05$, compared with LNCaP control cells. Values are mean ± SEM.

tion between AR^{v567es} and AR^{fl}, we sought to determine whether the interaction between the 2 ARs had an effect on mRNA stability or AR protein degradation. We examined *AR* mRNA stability following treatment with actinomycin D and found no differences between LNCaP pc and LNCaP AR^{v567es} cells (Figure 7B). We then determined whether the interaction of AR^{v567es} with AR^{fl} affected AR protein degradation. When translation was halted with cycloheximide, there was a slowing in degradation of the AR^{fl} in cells containing both receptors, particularly in the presence of DHT, when compared with cells with only the endogenous AR receptor (Figure 7, C and D). These data are also consistent with studies showing that AR activation increases AR protein through increased translation efficiency and a decrease in the rate of AR degradation (16).

Targeting full-length and variant AR expression with the histone deacetylase inhibitor SAHA. Since the AR^{v567es} does not contain a LBD, androgen ablation has no effect on signaling. Thus, in tumor cells expressing AR^{v567es}, alternative approaches for abrogating AR signaling will be required. The histone deacetylase inhibitor SAHA has been shown to alter levels of AR protein by inhibiting AR transcription (15). Therefore, we grew LNCaP pc and LNCaP AR^{v567es} cells in vitro to 80% confluence with either CS serum or with CS serum plus DHT. SAHA was then added to the medium at the concentrations indicated in Figure 8A. In the absence of DHT, SAHA markedly decreased AR^{fl} expression in LNCaP pc cells and AR^{v567es} and endogenous AR^{fl} in the LNCaP AR^{v567es} cells. However, in the presence of DHT, SAHA only effectively decreased AR^{fl} expression and had a minimal effect on AR^{v567es} expression. In order to

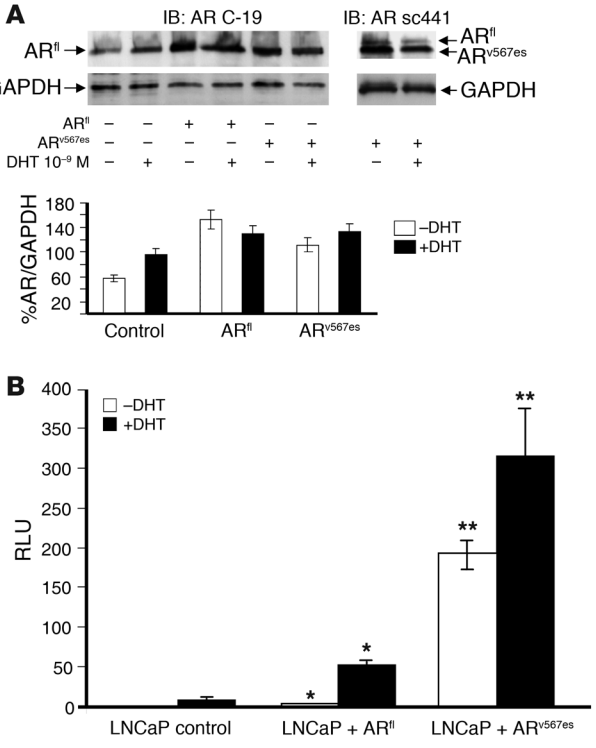

Figure 5

AR^{v567es} increases endogenous AR^{fl} expression and activity to similar levels as overexpression of AR^{fl} in LNCaP cells. (**A**) Western blot of LNCaP cells transfected with empty vector, AR^{fl}, or AR^{v567es}. Immunoblot with AR C-19 antibody, which only detects AR^{fl}. Note the increase in AR^{fl} following transfection with either AR^{fl} or AR^{v567es} compared with empty vector control. The panel on the right shows immunoblot using AR sc441 antibody to demonstrate presence of AR^{v567es} in LNCaP AR^{v567es} cells. The graph depicts relative amounts of AR^{fl} present, using LNCaP pc plus DHT as the baseline. Values are mean ± SEM. (**B**) ARR3-Luc reporter assay on cell lines from **A**, grown with and without DHT (10^{-9} M). Note that for the LNCaP pc cells, DHT resulted in more than a 10-fold increase ($P < 0.01$) in reporter activity compared with baseline. This increase in activity is difficult to discern in this figure due to the scale used to show changes with the AR^{v567es} construct. Values are mean ± SEM. *$P < 0.01$, LNCaP AR^{fl} cells compared with LNCaP control cells with same treatment; **$P < 0.001$, LNCaP AR^{v567es} cells compared with LNCaP AR^{fl} cells with same treatment.

determine whether this same effect of androgens would occur on tumors that were resistant to castration and in which the primary AR consisted of AR^{v567es}, we cultured LuCaP 86.2 tumors in vitro and treated the cells with SAHA or SAHA plus DHT. SAHA was effective at decreasing AR^{v567es} in the presence and absence of DHT (Figure 8, B and C). Although SAHA decreased AR^{v567es} protein levels in the LuCaP 86.2 cells, the resulting decrease in growth (Figure 8D) cannot be conclusively attributed to loss of AR^{v567es}, since histone deacetylases have multiple effects on cells that result in suppression of cell proliferation (17, 18).

AR^{v567es}-regulated gene expression. In order to compare and contrast the gene expression program regulated by *AR^{v567es}* and AR^{fl}, we first measured transcript abundance changes in LNCaP cells expressing AR^{fl} following exposure to androgen. Cells were grown in CS serum, with or without 10^{-9} M DHT, for 24 hours in triplicate. Following RNA isolation, transcript abundance levels were measured using whole-genome microarrays. Because the magnitude of changes was quite high between the AR^{fl} CS and AR^{fl} DHT-treated groups, *t* test significance was set at a stringent *q* value of less than 0.01%. A separate experiment compared transcript abundance in LNCaP cells expressing AR^{fl} or AR^{v567es} grown in CS medium. Gene expression differences between AR^{fl} CS and AR^{v567es} CS groups were more subtle, and genes exhibiting *q* values of less than 10% were included in order to cross-compare similar numbers of gene expression changes between the experiments (Figure 9). We performed an analysis of Gene Ontology (GO) using the EASE software tool, which calculates overrepresentation statistics for GO terms in the significant list, with respect to all genes represented in the data set (Supplemental Tables 2 and 3, GO analysis statistics).

We determined that well-known androgen-regulated genes, such as *PSA*, *TMPRSS2*, and *FKBP5*, altered by DHT treatment in cells expressing AR^{fl}, were also altered in the context of AR^{v567es} expression in the absence of exogenous androgens, confirming the hypothesis that AR^{v567es} is capable of activating the AR-regulated gene expression program in the setting of castration. We further found that AR^{v567es} regulates a subset of genes that we believe to be unique that are not influenced by androgens in the context of the AR^{fl}. Analysis of GO terms enriched specifically in AR^{v567es} cells revealed that GO molecular function "transcription factor activity" is significantly increased in the absence of androgen, potentially signifying activation of other growth and survival pathways. Among the transcription factors upregulated by AR^{v567es} that are known to induce a proliferative program of gene expression were STAT3, which has antiapoptotic as well as proliferative effects, and JUN, which behaves as a positive regulator of cell growth by protecting cells from p53-dependent senescence and apoptosis (19–21). AR^{v567es} also activated genes involved in the metabolism of androgens. Interestingly, even in the absence of exogenous AR ligands, cells expressing AR^{v567es} demonstrated a signature of androgen metabolism, with enriched GO terms of biological processes "steroid biosynthesis" and "sterol metabolism." Such ligand-independent stimulation of steroidogenic pathways in AR^{v567es} cells may provide a survival advantage in a low-androgen environment.

In addition to differences in the genomic signaling programs between AR^{v567es} and AR^{fl}, our data also indicate that these variant receptors may differentially regulate other AR activities. In this context, AR^{v567es} altered components of IGF pathway signaling in a manner distinct from that of the AR^{fl}. IGF-IR expression was enhanced by ligand stimulation of AR^{fl}, whereas AR^{v567es} suppressed IGF-1R expression (Figure 4D and Figure 9B). Pandini et al. have shown that the AR stimulates IGF-IR expression through a nongenomic pathway, involving binding of AR^{fl} to Src and downstream activation of the transcription factor MAPK (22). Our cell-based localization studies indicated that AR^{v567es} was rapidly targeted to the nucleus and, during this process, facilitated the movement of AR^{fl} as well. Thus, AR^{v567es} may have a primary effect

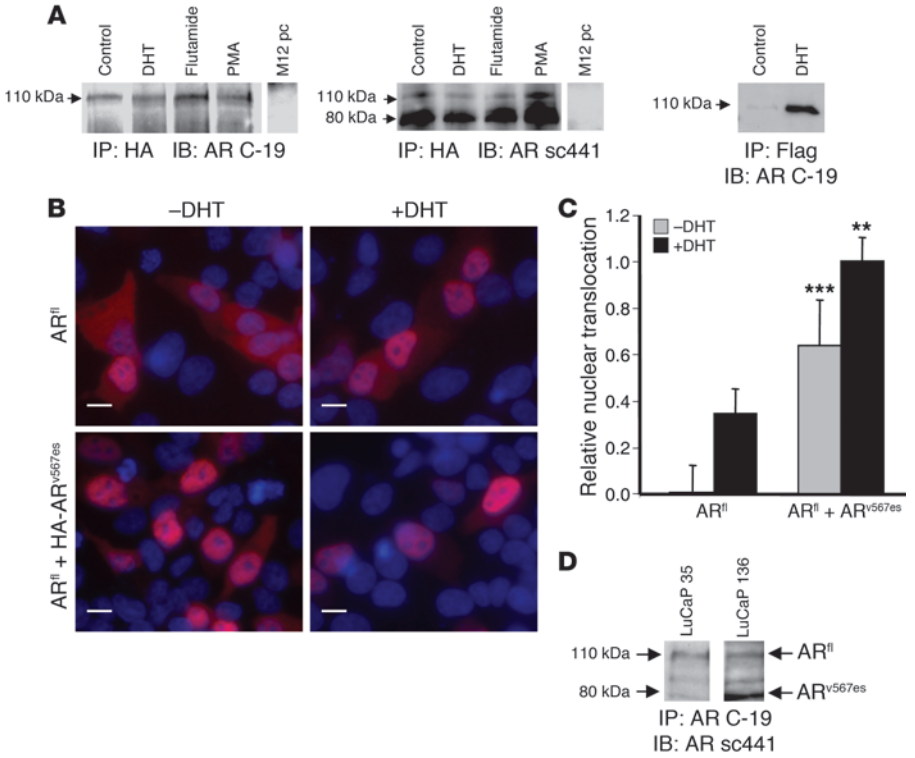

Figure 6

The splice variant AR^{v567es} forms a complex with AR^{fl}. (**A**) Immunoprecipitate with an HA antibody in M12 cells double transfected with AR^{fl} and HA-AR^{v567es}, followed by immunoblotting with AR C-19, which only recognizes AR^{fl}, and AR sc441, which recognizes both AR^{v567es} and AR^{fl}. As a positive control, Flag-tagged AR^{fl} was transfected into M12 cells and brought down with a Flag antibody. Lanes were run on same gel but were noncontiguous. (**B**) M12 cells transfected with the AR^{fl} construct alone or in combination with the HA-AR^{v567es} construct. Cells were grown in serum-free media and then treated with DHT 10^{-9} M or vehicle (EtOH). AR^{fl} was immunolabeled with the AR C-19 antibody (red) and nuclei were immunolabeled with DAPI (blue). In cells containing both AR^{fl} and AR^{v567es}, AR^{fl} translocates to the nucleus in the absence of ligand. Scale bar: 10 μm. (**C**) Relative quantitative nuclear translocation of AR^{fl}. A minimum of 100 AR-positive cells were included for each construct. For comparisons, the population with the lowest percentage of translocation was considered 0 (AR^{fl} with no DHT), and the population with the highest percentage of translocation was considered 1 (AR^{v567es} with DHT). Values are mean ± SEM. $^{**}P < 0.001$, $^{***}P < 0.0001$, compared with AR^{fl} with same treatment. (**D**) Tumor lysates were made from LuCaP 35 and 136 xenografts taken from castrated SCID mice, immunoprecipitated with AR C-19, and immunoblotted with AR sc441. AR^{v567es} was brought down with AR^{fl} in the LuCaP 136 xenograft.

through enhanced genomic AR activity and the concomitant suppression of nongenomic AR activity exerted by AR^{fl}.

AR^{v567es} enhances the growth of prostate cancer following ADT in vivo. Since AR^{v567es} is constitutively activated and also transactivates AR^{fl} in the absence of androgen, we next sought to determine whether AR^{v567es} influences prostate cancer responses to ADT in vivo. We implanted LNCaP AR^{v567es} cells or control LNCaP pc cells into immunocompromised *nu/nu* mice in subcutaneous locations. In the initial androgen-sensitive growth phase in eugonadal animals, there was no difference in tumor growth rate among the cell lines inoculated (data not shown). After tumors attained a size of approximately 0.2 cc, the mice were castrated, and tumor volumes were measured over a 13-week time period. We did not observe significant growth of the grafts comprised of LNCaP pc cells. However, grafts comprised of LNCaP AR^{v567es} cells were measurably larger than those of control cells by the 10-week time point (tumor volume of LNCaP pc vs. LNCaP AR^{v567es} cells; $P < 0.01$), and subsequent rapid growth required animal sacrifice by 13 weeks due to tumor size (Figure 10A). We examined the resulting tumors, resected at the study endpoint for AR transcript levels and splice variants. In the small LNCaP pc tumors surviving castration, transcript levels encoding AR^{fl} were not significantly different relative to levels in cells prior to castration, and the AR^{v567es} remained undetectable. In contrast, in LNCaP AR^{v567es} tumors the ratio of AR^{v567es} transcripts to those encoding AR^{fl} increased significantly from 0.5 to 4.3 ($P < 0.05$). These results support evolution of a tumor cell population favoring the selection of cells expressing higher levels of the AR^{v567es} variant.

We next examined the response of prostate cancers expressing endogenous AR^{v567es} to ADT. We chose 3 representative LuCaP xenografts, which have distinct differences in the expression of AR^{fl} and AR^{v567es} (Figure 10E). The LuCaP 35 xenograft expressed AR^{fl}, with little detectable AR^{v567es}. In addition, we have previously published that LuCaP 35 xenografts maintain high levels of intratumoral DHT following castration (1.7 ± 0.27 ng/g of tumor tissue precastration versus 1.5 ± 0.48 ng/g of tumor tissue after castration; ± SD; P = NS) (8, 9). The LuCaP 136 xenograft expressed AR^{fl} and had high intratumoral DHT levels (2.4 ± 0.9 ng/g) in eugonadal animals, but following castration there was a significant decrease in intratumoral DHT (0.15 ± 0.03 ng/g; $P < 0.001$) and increased expression of AR^{v567es} (Figure 10E). Finally, the LuCaP 86.2 xenograft, which had low levels of intratumoral DHT regardless of castration status (0.4 ± 0.04 ng/g precastration vs. 0.1 ± 0.04 ng/g after castration; $P < 0.05$), expressed primarily AR^{v567es} (Figure 10E). We implanted replicate xenografts subcutaneously into SCID mouse hosts, 24 animals per group, and after achieving a tumor volume of 0.2 cc, half of the animals in each group were subjected to ADT by surgical castration. Tumor responses correlated with the level of AR^{v567es} expression. No response to ADT was seen for the LuCaP 86.2 xenograft, which predominately expressed AR^{v567es} (Figure 10, B and E). The growth of LuCaP 136 tumors, which express a mix of AR^{fl} and AR^{v567es} following castration, was significantly suppressed following ADT, relative to eugonadal animals (14-week time point; $P < 0.01$), although there was a slow progressive increase in tumor volumes over time (Figure 10, C and E). LuCaP 35 tumors, which predominately express AR^{fl}, exhibited a sustained response to ADT, with minimal tumor growth measured over 14 weeks (Figure 10D).

Evolution of AR^{v567es} in prostate xenografts. Since AR^{v567es} is a splice variant and generation of the variant is posttranscriptional, acqui-

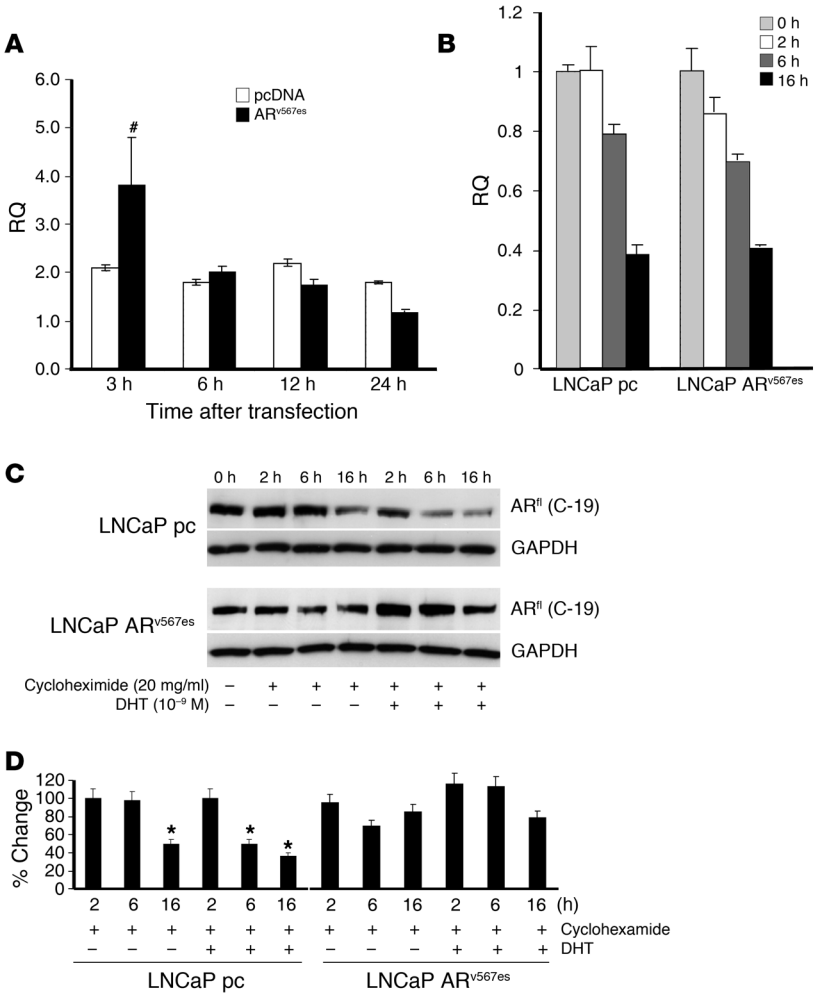

Figure 7
Stability of AR^{fl} in presence of AR^{v567es}. (**A**) LNCaP cells were transfected with either the empty vector (pcDNA) or the AR^{v567es} construct. After transfection, RNA was extracted from cells at the times noted, and qt-RT-PCR was performed for AR^{fl}. The relative levels of AR^{fl} at each time point were compared with levels at time 0 hours. Following transfection with the AR^{v567es} construct, there was an increase in *AR^{fl}* mRNA at 3 hours that rapidly returned to control levels by 6 hours after transfection. $^{\#}P < 0.05$ AR^{v567es} vs. pcDNA. Values are mean ± SEM. (**B**) PCR for AR^{fl} in actinomycin D–treated LNCaP pc and LNCaP AR^{v567es} cells. Note that AR^{v567es} did not significantly affect *AR^{fl}* mRNA stability. (**C**) The Western blot of cycloheximide-treated LNCaP pc and LNCaP AR^{v567es} cells demonstrates that AR^{v567es} increases AR^{fl} protein stability in the presence of DHT. (**D**) Graph depicting relative protein levels of AR^{fl} following treatment with cycloheximide in LNCaP pc versus LNCaP AR^{v567es} cells. $^{*}P < 0.01$ versus 2 hour time point. Values are mean ± SEM.

sition of AR^{v567es} by the prostate could be considered an adaptive mechanism rather than a selected event, such as those encoded by a mutation in AR DNA. This would appear to be the case for the LuCaP 136 and 86.2 xenografts. When we evaluated the original tissue specimens from which these xenografts were derived, ascites cells and a bladder metastasis, respectively, only *AR^{fl}* mRNA was present in the original LuCaP specimen, whereas both *AR^{fl}* and *AR^{v567es}* mRNA were present in the LuCaP 86.2 original specimen (Supplemental Figure 2). This finding was consistent with the LuCaP 136 xenograft initially responding to castration in the mouse, but the 86.2 xenograft having no response. However, after castration and continued passage in SCID mice, *AR^{v567es}* mRNA became the dominant *AR* mRNA in the LuCaP 86.2 xenograft, and *AR^{v567es}* mRNA was generated in the LuCaP 136 xenograft (Supplemental Figure 2 and Figure 10E). Further, as mentioned earlier, in those LuCaP xenografts with pairs of castrate-sensitive and castrate-resistant tumors, there was a significant increase in AR^{v567es} expression in the castrate-resistant tumors compared with castrate-sensitive tumors (Figure 1). These data indicate that the generation of the splice variants is a dynamic process that occurs in response to castration pressures exerted on the AR signaling program.

AR splice variants are rarely expressed in benign prostate epithelium, and levels are increased in men with prostate cancer. To further evaluate the contribution of the AR^{v567es} variant to prostate cancer, we investigated the distribution of the AR splice variants directly in normal and neoplastic human prostate epithelium. We first acquired benign prostate epithelium by laser-capture microdissection (LCM) from prostate biopsies of 36 normal men, without evidence of prostate cancer, enrolled in a study of male contraception (acycline or DHT gel). Using quantitative RT-PCR (qt-RT-PCR) to quantitate transcripts isolated from benign epithelium, we were able to detect mRNAs encoding AR^{fl} in 35 subjects, and 6 out of 36 (17%) men expressed AR^{v567es}, 2 out of 36 (6%) men expressed the recently described AR splice variant termed AR-V7, and 1 out of 36 (3%) men expressed the AR splice variant termed AR3 (13, 14) (Table 1 and Figure 11A). The men who expressed AR variants, while they did not have prostate cancer, had either been castrated using the LHRH receptor antagonist acycline or had tissue androgens suppressed by administration of DHT gel.

Since we found AR^{v567es} in our group of normal men, we next evaluated whether in primary (untreated) prostate cancer specimens the variant was in the malignant epithelium, benign epithelium, or both; if primarily in the malignant epithelium, this might suggest that the presence of a variant was etiologic in cancer development. Therefore, we examined cDNA from laser-captured, matched benign and malignant epithelium of primary prostatectomy tissue. We found that the variants were expressed in both benign and malignant prostate epithelial tissue (Figure 11A).

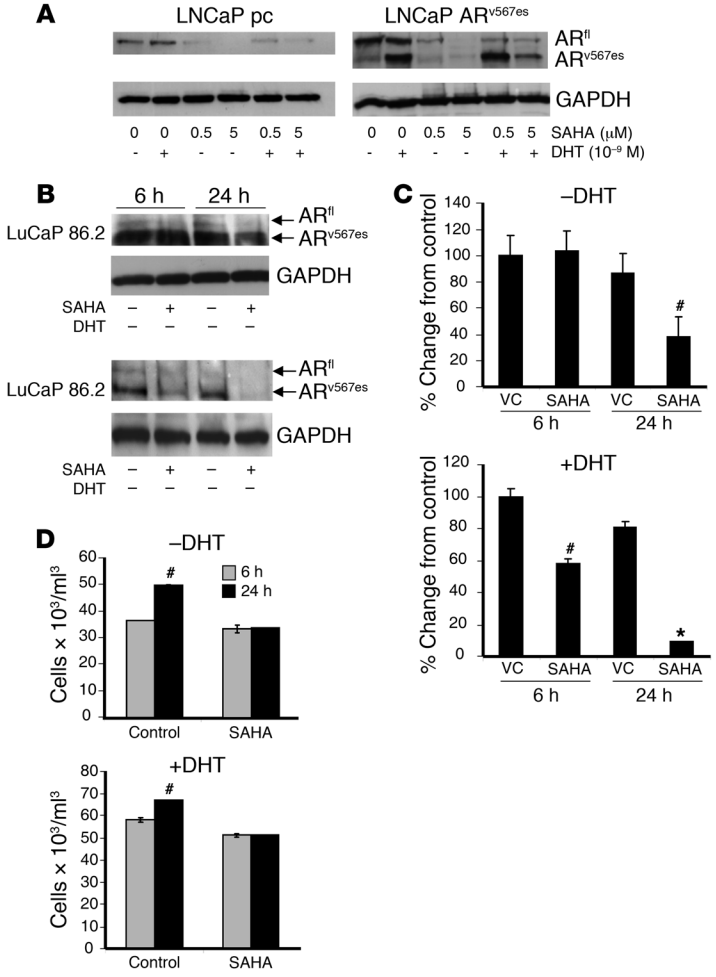

Figure 8
The effect of the histone deacetylase inhibitor, SAHA, on AR^{v567es}-expressing cells. (**A**) LNCaP pc or LNCaP AR^{v567es} cells were grown to 80 percent confluence in CS medium, with or without DHT (10^{-9} M). SAHA was then added at the concentrations noted, and after 16 hours, cell lysates were collected, and Western blots were run with AR sc441 primary antibody, which detects both full-length and variant AR. (**B**) Two LuCaP 86.2 xenografts were removed and digested with collagenase to single cell suspensions. Cells were then plated in RPMI 5% CS medium, with or without DHT (one xenograft was grown with DHT, another without). Six hours later, cells were treated with either vehicle control (VC) or SAHA (5 mM). Six and twenty-four hours following treatment, cells were trypsinized and counted and cell lysates were collected for Western blots (blotted with AR sc441 antibody or GAPDH as a loading control). (**C**) Density of AR^{v567es} bands corrected for GAPDH. $^{\#}P < 0.05$, $^{*}P < 0.01$, compared with vehicle control 6 or 24 hours. Values are mean ± SEM. (**D**) Cell counts corresponding to treatments in **B**. $^{\#}P < 0.05$, compared with 6 hour control. Values are mean ± SEM.

These data suggest that the presence of AR variants is not necessarily etiologic in the initiation of prostate cancer.

Variant AR expression in prostate cancer metastases. To determine the frequency of AR splice variant expression in advanced prostate cancers, we successfully amplified cDNA from 69 metastases, derived from 13 patients undergoing a rapid necropsy for tumor acquisition. All of these patients were documented to have either surgical or chemical castration, with tumor progression to a clinical state of CRPC. Tumor tissue was isolated by laser-assisted microdissection, and RNA integrity was verified. Despite amplification of GAPDH, no full-length or variant AR expression was detected using RT-PCR in 23 samples. These 23 metastases were from patients whose primary tumors had a neuroendocrine phenotype and would not be expected to depend on functional AR. Of the remaining 46 metastases, 37 out of 46 (80%) expressed AR^{fl}, 20 out of 46 (43%) expressed AR^{v567es}, 11 out of 46 (24%) expressed AR-V7, and 3 out of 46 (6%) expressed AR3 (Table 1 and Figure 11B). Interestingly, 9 out of 46 (20%) metastases expressed only the AR^{v567es} variant, but expression of AR-V7 or AR3 occurred concomitantly with AR^{fl} expression. Overall, 27 out of 46 (59%) AR-positive metastases expressed one or more AR splice variants. When evaluating all of the metastases from each individual patient collectively, 12 out of 13 patients had at a minimum one metastasis that was positive for at least one AR splice variant, and 10 out of 13 patients had at a minimum one metastasis that was positive for AR^{v567es}. Further, the presence of an AR variant was clustered among patients. For example, the majority of metastases for one patient may have been positive for a variant, whereas a different patient may have very few metastases that were positive for that variant. No patient had all samples positive for the same AR variant.

Discussion

The progression of prostate cancer to an AR-independent state has recently become regarded as a misnomer (8–10, 23). Transcriptional activation of the AR has been suggested to occur through several nonsteroidal factors, such as IL-6, EGF, integrins, and insulin-like growth factors as well as by increased expression of AR cofactors (3, 24–29). Another mechanism for AR-regulated prostate cancer progression following castration is an alteration in AR protein. This alteration has been reported to occur by genomic mutations: either ligand-dependent activating mutations or ligand-independent activating mutations (12). Genomic mutations in the AR are not common, but those that result in an AR that functionally increases AR activity and lead to CRPC are even less common. Recently, constitutively active posttranslational splice variants of the AR have been reported in human prostate cell lines, xenografts, and human tissues (13, 14, 30).

In this paper, we describe a splice variant of the AR that we believe to be new, in which exon 4 has been spliced to exon 8, and thus, exons 5, 6, and 7 have been deleted. This alternative splicing

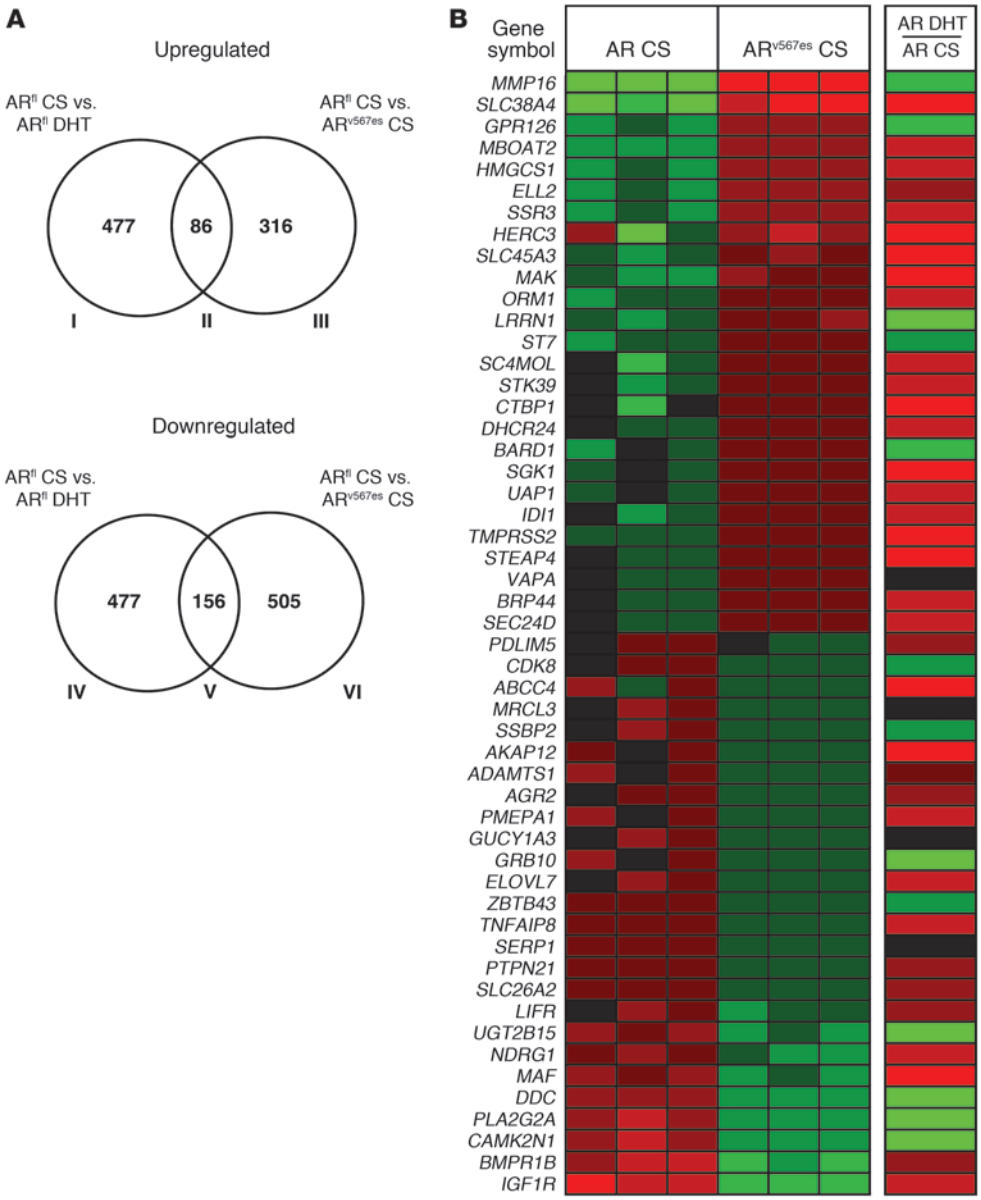

Figure 9
Expression profiles of LNCaP pc and LNCaP AR^{v567es} cells. (**A**) Venn diagrams showing the gene number per comparison for expression profiles of androgen-regulated and AR^{v567es}-regulated genes in LNCaP cell lines. Cells were grown in CS medium with or without DHT (10^{-9} M) for 24 hours, in triplicate experiments. Microarray analysis using Agilent 44K whole human genome expression oligonucleotide microarray slides was performed. Statistical analysis was conducted using 2-sample, unpaired *t* test with the SAM software, with a *q* value of less than 0.01% considered statistically significant for AR^{fl} cells and a *q* value of less than 10% considered statistically significant for AR^{v567es} cells. I and IV indicate genes upregulated or downregulated by DHT in LNCaP cells; II and V indicate genes upregulated or downregulated by DHT in LNCaP cells or LNCaP AR^{v567es} cells compared with LNCaP cells with no DHT; and III and VI indicate genes regulated by AR^{v567es} in LNCaP cells compared with LNCaP cells without DHT. (**B**) The top AR-regulated genes in the LNCaP AR^{v567es} cells compared with LNCaP controls grown in CS medium. Note that the right hand column shows changes in genes previously described to be regulated by DHT in LNCaP cells. Results of GO analysis of genes upregulated or downregulated by DHT in AR cells or genes uniquely upregulated or downregulated in AR^{v567es} cells are listed in Supplemental Tables 2 and 3.

event leads to a frame shift, so that 10 amino acids that we believe to be unique are encoded for and followed by a stop codon, resulting in an AR variant protein that is 180 amino acids shorter than the AR^{fl} protein. Thus, this variant, unlike the previously reported AR splice variants, retains the hinge region, which is necessary for complete nuclear translocation of the AR (31). Similar to previously reported AR splice variants, we show that the AR splice variant produced by this event is constitutively active (13, 14, 30). Unlike other reports, though, in which variants were cloned using a 3′ RACE method in a prostate cancer cell line or in which the authors created potential deletion mutants based on the different splicing sites in the AR, we identified AR^{v567es} through the analysis of 25 distinct human prostate xenografts. We originally sequenced the ORF of the AR in the xenografts using 2 sets of PCR primers, as described. Since these primers detect the predominant *AR* mRNA species, 2 of the xenografts, 86.2 and 136, had the splice variant as the majority of their AR. When specific primers were designed to detect the 4–8 junction present in AR^{v567es}, the variant was found in several additional xenografts. We also noted that in the same xenograft, the level of the AR^{v567es} was not constant and varied depending on passage number. When we examined the primary human tumors from which the LuCaP 86.2 and 136 xenografts were developed, we noted that the variant AR had always been present in LuCaP 86.2, while in LuCaP 136 the AR^{fl} was the predominate receptor. However, the AR variant became more predominant in the LuCaP 136 xenograft following long-term growth in mice as well as after it was grown in castrated mice. These data suggest that the level of splice variant AR is not fixed but is dynamic and likely regulated by environmental factors, including decreasing androgen levels (12, 13).

We expressed this new AR variant in both benign and prostate cancer cell lines and found that AR^{v567es} functions like a constitutively active AR in both types of cells and is resistant to the effects of flutamide on AR activity. Further, we report that in cells express-

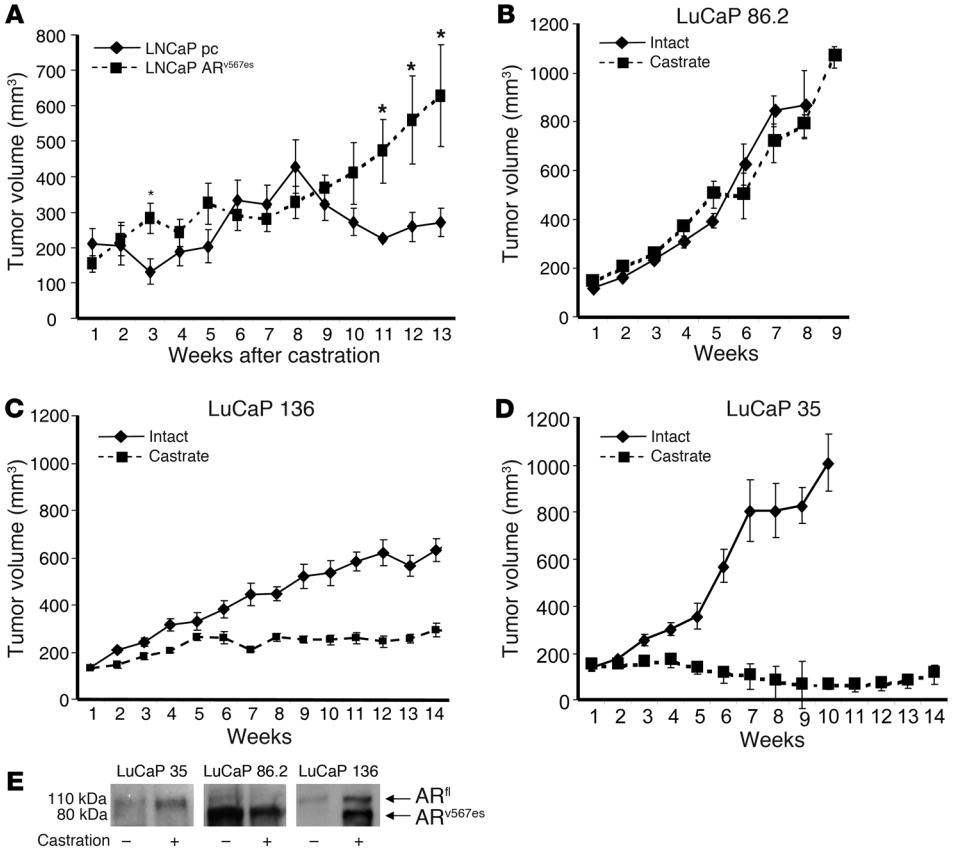

Figure 10

Tumor growth of LNCaP AR^{v567es} cells and xenografts expressing various amounts of AR^{v567es}. (**A**) 1×10^6 LNCaP pc or LNCaP AR^{v567es} cells were mixed 1:1 with Matrigel and injected s.c. into athymic nude mice (n = 10 per line). When tumors reached a volume of 100–200 mm^3, mice were castrated and animals were followed until tumors regrew and reached a volume of 1,000 mm^3 or met IACUC criteria for euthanasia. There was no difference in growth rate in intact mice. Following castration, the LNCaP AR^{v567es} tumors, which did not decrease in volume following castration, grew to a significantly larger volume, more quickly than those of controls. *P < 0.01, LNCaP AR^{v567es} tumor volume versus LNCaP pc tumor volume. Values are mean ± SEM. (**B**–**D**) The response of tumor volume to castration in 3 different xenografts (intact, n = 12 per xenograft; castrate, n = 12 per xenograft). Note that LuCaP 86.2, which has the majority of its AR in the AR^{v567es} form, had no castration response; LuCaP 136, which has both full-length and variant AR, had a modest response to castration; and LuCaP 35, which has the majority of its AR as AR^{fl}, had a marked decrease in tumor volume in response to castration. Values are mean ± SEM. (**E**) Western blots of representative xenografts before and 6 weeks after castration using AR sc441, which recognizes AR^{v567es} and AR^{fl}. Lanes were run on different gels.

ing endogenous AR^{fl}, AR^{v567es} increases the level of endogenous receptor by slowing the rate of protein degradation.

Since a constitutively active AR could lead to the progression of the tumor after castration, we examined expression of the AR^{v567es} variant in specimens of prostate cancer from men who had died from their cancer. All of these men were castrated at the time specimens were obtained; while a third of the samples did not have any detectable AR, over 50% of the specimens that contained detectable AR transcripts were positive for one or more of the constitutively active variants. These included biopsies from the prostate as well as lymph node, lung, liver, and bone. Interestingly, the presence of AR^{v567es} was not distributed randomly among the patients but rather the variant clustered within a patient's specimens. Further, not all specimens within a patient were positive for an AR variant, consistent with a hypothesis of ongoing splicing activity that generates AR variants. We also examined specimens for the presence of 2 other AR variants recently reported to affect survival in prostate cancer, AR3 and AR-V7 (13, 14). AR^{v567es} was the most common of the 3 variants examined and several specimens contained more than one AR variant. Additionally, nearly all of the specimens that contained one or more of the variants also contained a AR^{fl}. These findings are not surprising, since there are multiple mechanisms by which the AR continues to be activated following castration.

Since AR splicing is determined in part by differences in androgen levels, we asked whether the splice variants might be present in men without cancer and in benign epithelium in men with cancer. In young men, ages 35–55, with normal PSA levels of less than 2.0 ng/ml and no clinical evidence of prostate cancer, who had a prostate biopsy as part of their participation in a male contraceptive study, we found that the AR^{v567es} variant was occasionally expressed in prostate epithelium of men receiving treatment but not in men receiving placebo. In a separate set of non-castrate older men, ages 59–70 years, who had a radical prostatectomy for prostate cancer, analysis of paired laser-captured benign and malignant prostate epithelial samples showed that AR splice variants could be found in benign, malignant, or both specimens from the men. These data suggest that expression of AR variants is not necessarily etiologic in cancer development, but if AR variants are present, they might serve to facilitate progression when hormone suppression is applied. This phenomenon has been demonstrated in a mouse model (32) as well in our current data, using various human xenografts grown in castrated versus intact SCID mice.

In this paper, we have shown that some prostate tumors may express only the variant AR receptor. However, while expression of AR splice variants is of interest and their functions have been examined as specific entities, the vast majority of splice variants are expressed in cells, along with a full-length receptor. Dimerization of full-length receptors occurs through both AF1 and AF2 sites as well as other N-terminal/C-terminal (N/C) interactions (33). Whereas most steroid receptors require the N/C interaction for binding of cofactors and subsequent receptor activation, the AR is unique in

Table 1
Number of metastases positive for AR^{fl} or AR splice variants

AR examined	Normal tissue samples ($n = 36$)	Metastasis samples ($n = 69$)
AR (full-length or variants)	35	46
AR^{fl}	35	37
AR^{v567es}	6	20
AR-V7	2	11
AR3	1	3
AR^{v567es} and AR-V7	0	6
AR^{v567es} and AR3	0	0
AR^{v567es}, AR-V7, and AR3	0	0
AR-V7 and AR3	1	1

that the AR AF2 domain has evolved such that it preferentially interacts with FxxLF-like motifs contained in the AR N-terminal domain (23FQNLF27 and 433WHTLF437) over LxxLL-like motifs in the coregulatory proteins' amino termini. As such, an AR lacking the LBD is still active, but now ligand cannot induce dimerization (33).

Although we and others have shown the constitutive function of the AR variants independent of AR^{fl}, the majority of tumors express both ligand-dependent and constitutively active splice receptors. In this study, we believe that we have shown for the first time that a constitutively active AR splice variant, AR^{v567es}, interacts with AR^{fl}. We demonstrated that we could pull down variant AR with AR^{fl}, not only in prostate cancer cells lines in which we overexpressed the variant, but also in human xenografts that endogenously express both full-length and variant AR protein. Further, we show that the variant causes translocation of the AR^{fl} in the absence of ligand, which results in enhanced AR transcriptional activity and increased cell proliferation in response to very low concentrations of ligand. However, the characterization of where the splice variant binds and interacts with AR^{fl} has yet to be determined.

Recent studies and data we presented here have shown that after standard androgen ablation, such as castration, levels of androgen in the prostate are still measurable. In our studies, using a panel of human xenografts that we believe to be unique, we further show a strong correlation between increased expression of the different AR variants in tumors and low intratumoral levels of androgens. In particular, the AR^{v567es} is expressed most abundantly in tumors with the lowest levels of androgens. Thus, the expression of the AR variants, including the AR^{v567es} variant that we believe to be unique, provides a mechanism to enable cancer progression in the face of decreased androgens.

AR^{v567es} contains the entire DNA-binding domain and nuclear localization sequence (Supplemental Figure 1). It is clear that AR^{v567es} is constitutively active and can function without ligand or

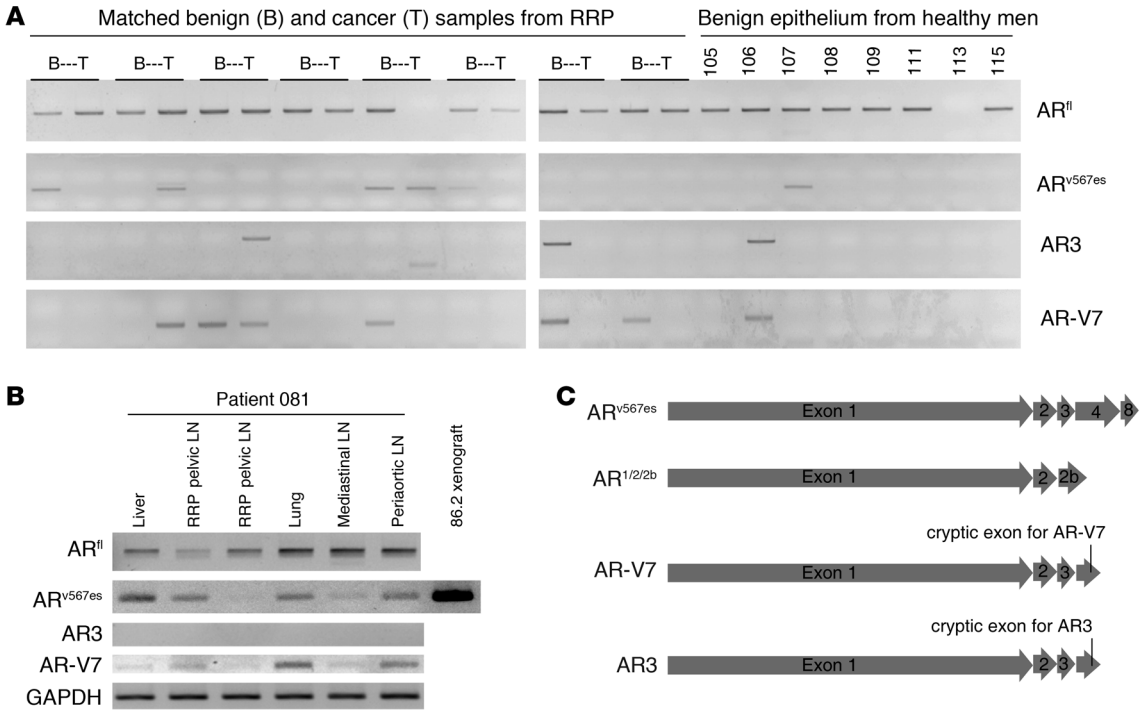

Figure 11
Expression of the splice variant AR^{v567es} in human prostates. (**A**) AR variant PCR products from laser-captured samples of benign (B) and malignant tissue (T) from prostate tissue obtained at the time of prostatectomy from non-castrate men. Note that tumor or benign tissue may be positive in these samples. Samples 105–115 are PCR products from men, aged 35–55 years, with no evidence of prostate cancer, who were enrolled in a male contraception study. (**B**) Results of variant AR PCR products from metastases in a man who died from his prostate cancer. Table 1 shows results for all metastases samples. Variants include the AR^{v567es} described in the current report and 2 variants previously described, AR3 and AR-V7. GAPDH was used as a control for adequacy of RNA in the sample. Primers are described in the Methods section. If GAPDH could not be amplified, the sample was not included in the study. Inverted agarose images are shown for **A** and **B**. (**C**) Diagram of AR^{v567es} variant compared with previously published AR variants ($AR^{1/2/2b}$ in ref. 30; AR-V7 in ref. 14; and AR3 in ref. 13). RRP, radical retropubic prostatectomy.

AR^{fl}. On the other hand, we have also shown that AR^{v567es} can form a heterodimer with AR^{fl} and enhance its activity (Figure 4). Thus, for the first time to our knowledge, we show that a constitutively active AR variant generated by castration in human tumors may function in a ligand-independent manner or enhance the ligand-dependent function of the AR^{fl}. Either one or both of these mechanisms may be active in a tumor cell when both variant and AR^{fl} coexist.

Since AR^{v567es} does not bind ligand and has no N/C interaction, it might be expected that its interaction with AR coregulators and its binding to androgen response elements (AREs) may be altered. We have shown the latter in this study, since we saw enhanced activation of ARE-containing reporter constructs in cells overexpressing AR^{v567es} compared with cells simply overexpressing AR^{fl}. Further, in cells expressing AR^{v567es}, we observed a decrease in genes that are upregulated via the nongenomic pathway, including IGF-1R. This would suggest that the repertoire of genes activated by the splice variant receptors will have similarities and differences with that of the full-length ligand-dependent AR. In this study, we have seen that there are significant differences in profiles of androgen-regulated genes in LNCaP cells that only express the endogenous AR and those that express the splice variant, even when androgens are added to the culture medium of the control LNCaP cells. These differences in gene expression by cells that express the AR splice variants may be significant, because the AR has tumor-promoting and -suppressing properties. Since the AR splice variants are associated with cancer progression, the differences in gene expression may help to delineate those AR-regulated genes involved in tumor progression.

Using data from the gene arrays comparing xenografts with high and low levels of expression of the AR^{v567es} variant, we were able to identify a panel of splicing factors that were differentially expressed. Specific regulation of these factors by androgens has not been determined, although several of the factors have been implicated in generating variability of prostate tumors (34–37). If specific splicing factors can be identified that generate these AR splice variants, inhibition of these factors at the time of androgen ablation could significantly enhance the effects of androgen ablation and prevent or delay development of castration-resistant disease.

In summary, we demonstrate in this report that AR splice variants that contribute to castration resistance are common in prostate cancer. There appears to be a family of AR variants, generated after androgen ablation, that results in a constitutively active AR. Identification of these variant receptors may serve as a biomarker for men destined for early recurrence and who are candidates for therapy directly targeting the AR rather than ligand.

Methods

Cell lines and xenografts. The generation and characterization of the M12 prostate cell line has been described previously (38–41). M12 cells were cultured in RPMI 1640 medium supplemented with 5% FCS, 10 ng/ml EGF, 0.02 mM dexamethasone, 5 μg/ml insulin, 5 μg/ml transferrin, 5 ng/ml selenium, fungizone, and gentamicin at 37°C with 5% CO_2. The androgen-sensitive LNCaP line was a gift from Robert Sikes (University of Delaware, Newark, Delaware, USA). These cells were grown in T-medium (Invitrogen) supplemented with 10% FBS, 100 units/ml penicillin, and 100 μg/ml streptomycin at 37°C with 5% CO_2. The generation of several of the LuCaP xenografts has been described previously (8, 14, 30, 42–45). The origin and characteristics of all 25 xenografts are included in Supplemental Table 1. These xenografts fail to grow as cell lines and do not survive freezing, thus they are maintained by serial passage in SCID mice. The LuCaP 86.2 xenograft is the exception and will grow in vitro for up to a month. LuCaP 86.2 xenografts were removed from animals and digested using collagenase digest buffer, as previously described (46). Dissociated cells were then plated down in RPMI medium plus 10% FBS.

Human tissue acquisition. Human primary and metastatic prostate tissues were obtained as part of the University of Washington Medical Center Prostate Cancer Donor Autopsy Program, which is approved by the University of Washington Institutional Review Board. Details of this program have been described previously (47, 48). The Institutional Review Board of the University of Washington Medical Center approved all procedures involving human subjects, and all subjects signed written informed consent. Prostate tissue samples from 36 healthy subjects without prostate cancer were obtained from men enrolled in a clinical trial of medical castration (n = 8) or DHT administration (n = 28) performed at the University of Washington (9) (ClinicalTrials.gov numbers NCT00161486 and NCT00161486, respectively). These studies were comprised of young men, ages 35–55 years, with normal PSA levels of less than 2.0 ng/ml and no clinical evidence of prostate cancer, who had a prostate biopsy as part of their participation in the respective studies. Transrectal ultrasound-guided prostate biopsies of the peripheral zone were immediately embedded in OCT compound (TissueTek OCT Compound, Sakura Finetek) and snap frozen in liquid nitrogen. Under a University of Washington institutional protocol for the use of excess tissue after surgery, 8 matched samples of benign and tumor prostate tissue were obtained from eugonadal patients undergoing radical prostatectomy for localized prostate cancer (49, 50). In addition, benign prostate tissue was obtained from 2 patients undergoing cystoprostatectomy unrelated to prostate cancer. An H&E-stained section of each sample was examined microscopically and none of these demonstrated cancer.

Cloning and sequencing of AR variant transcripts. To detect AR splice variants in human prostate tissues, prostate biopsy samples embedded in OCT were used for LCM. Approximately 2,000 to 3,000 epithelial cells per sample were collected from 8-μm sections using the Arcturus Veritas Laser Capture Microdissection System, according to the Arcturus PicoGene LCM Frozen Section Staining Kit protocol. Total RNA was isolated using the RNeasy kit (Qiagen), followed by treatment with DNase using the Qiagen RNase-Free DNase Set. RNA was quantitated in a Gene-Spec III spectrophotometer (Hitachi), and RNA integrity was evaluated using gel electrophoresis. Total RNA from xenografts and cell lines was isolated with RNA STAT-60 (Tel-Test). cDNA was synthesized using SuperScript First-Strand Synthesis System (Invitrogen). PCR was performed using Takara High Fidelity Taq polymerase with the following primers: hAR1113 forward, 5′-AGGATGGAAGTGCAGTTAGGGCT-3′; hAR2974 reverse, 5′-CATTTCCGAAGACGACAAGATGG-3′; hAR2695 forward, 5′-GGATGGATAGCTACTCCGGACCTTACG-3′; and hAR3973 reverse, 5′-CAAGGCACTGCAGAGGAGTAGTGCAGAG-3′. PCR products were subjected to sequencing analysis using the Applied Biosystems 3730XL DNA Analyzer. Betaine (Sigma-Aldrich) was added in PCR and sequencing reactions to a final concentration of 1 M to facilitate the amplification of the AR GC-rich region.

PCR of AR^{fl} was performed using the following primer pair: hAR3619 forward, 5′-ACATCAAGGAACTCGATCGTATCATTGC-3′, and hAR3832 reverse, 5′-TTGGGCACTTGCACAGAGAT-3′. The AR splicing variant, AR^{v567es}, was detected with the following primer pair: hARv567es forward, 5′-CCAAGGCCTTGCCTGATTGC-3′, and hAR3832 reverse, 5′-TTGGGCACTTGCACAGAGAT-3′. All primers were designed using the human *AR* mRNA reference sequence (GenBank NM_000044). We have submitted the novel AR splice variant mRNA sequence to GenBank (ARv567es; GenBank GU208210).

Vector constructs and cell transfections. cDNA of AR^{fl} (AR20) was cloned into pcDNA3 as described previously (41). cDNA of the entire AR^{v567es} vari-

ant was amplified by PCR from the LuCaP 86.2 xenograft cDNA, using primer pair hAR1113 forward, 5′-AGGATGGAAGTGCAGTTAGGGCT-3′, and hAR3973 reverse, 5′-CAAGGCACTGCAGAGGAGTAGTGCAGAG-3′, and subcloned into pcDNA3.1 after sequence confirmation. The human influenza hemagglutinin–AR (HA-AR) variant construct was generated by inserting a HA linker into the *Bam*HI site of the pcDNA-AR^{v567es} construct. The HA linker sequences are as follows: HA-s, 5′GATCCATGTACCCATACGATGTTCCAGATTACGCT3′, and HA-as, 5′GATCAGCGTAATCTGGAACATCGTATGGGTACAT3′. These expression constructs were transfected into the human prostate cancer cell lines M12 and LNCaP and the benign immortalized human prostate cell line P69 with Lipofectin 2000 (Promega), according to the manufacture's protocol. Stable clones were obtained with G418 selection (400 mg/ml), and the expression of AR^{fl} or AR^{v567es} was confirmed by RT-PCR and Western blotting.

Luciferase assays. Luciferase assays were performed as previously described using IGF-IR–LUC–, ARR3-probasin-LUC–, and PSA-LUC pGL3-LUC–based reporters (51, 52).

Determination of nuclear AR translocation. M12 cells were grown on glass coverslips on 12-well plates and transfected with pcDNA-Flag-AR^{fl} alone or cotransfected with pcDNA-Flag-AR^{fl} and pcDNA-HA-AR^{v567es}. Twenty-four hours after transfection, cells were treated for an hour with 10^{-9} M DHT, then fixed with cold 4% formaldehyde, and stained with anti-AR (C19) primary antibody and subsequently with Alexa Fluor 594–conjugated secondary antibody. Cells were counterstained with DAPI. Cells were imaged with an Applied Precision DeltaVision Microscope. AR nuclear translocation was measured by using software Cyteseer 2.0 (Vala Sciences Inc). AR translocation was determined by the ratio of total integrated intensities of the red channel on the nuclear mask (DAPI-stained area) divided by total integrated intensities of the red channel on the whole cell mask. At least 100 cells were analyzed in each group. All measurements were subtracted from the baseline condition (the population with the smallest percentage of cells demonstrating nuclear localization) and then compared with the population demonstrating the highest percentage of cells with nuclear localization.

Coimmunoprecipitation and Western blotting. Cells were lysed in cold lysis buffer (50 mM HEPES, 150 mM NaCl, 1.5 mM $MgCl_2$, 1 mM EGTA, 1% Triton X-100) with Complete Protease Inhibitors (Roche Applied Science). Precleared cell lysate was incubated with the anti-HA antibody (Santa Cruz Biotechnology Inc.) and ultralink immobilized protein A/G plus (Pierce). Immune complexes were separated by SDS-PAGE and transferred onto a nitrocellulose membrane for Western blotting detection of AR. Antibodies AR sc441 and C-19 (Santa Cruz Biotechnology Inc.), specific for the N terminus and C terminus, respectively, of AR^{fl}, were used for detection of AR. For Western blot analysis of cell lysates, cells were washed with PBS and lysed with cold lysis buffer containing Phosphatase Inhibitor Cocktail II (Sigma-Aldrich) and proteinase inhibitors (Complete Mini Tablets, Roche). Twenty-five micrograms of protein were resolved on 4%–15% SDS-PAGE, transferred onto a nitrocellulose membrane, and probed with respective antibodies. The blot was washed and incubated with a horseradish peroxidase–conjugated secondary antibody (Pharmacia Biotech) for 1 hour. Immunoreactive proteins were detected by ECL (Pharmacia Biotech). The membranes were stripped for 30 minutes in Stripping Buffer (Pierce) and reprobed with anti-GAPDH antibody as a loading control (Chemico) as described above. Independent experiments validated that this stripping procedure did not lead to loss of signal.

AR mRNA stability assay. LNCaP pc and LNCaP AR^{v567es} stable cells were treated with actinomycin D (10 mmol/l) for 0, 2, 6, or 16 hours. Equal amounts of RNA were analyzed for AR^{fl} and AR^{v567es} by real-time PCR (normalized using internal GAPDH control).

AR protein degradation assay. To determine whether AR^{v567es} changes AR^{fl} degradation, we used cycloheximide to inhibit new protein synthesis and assess AR protein stability. LNCaP pc cells and LNCaP AR^{v567es} stable cells were treated with 20 μg/ml cycloheximide for 0, 2, 6, or 16 hours. Cell lysates were collected and Western blotted with AR C-19 antibody, which recognizes the AR C terminus (Santa Cruz Biotechnology Inc.).

Microarray gene expression quantitation. Total RNA from experimental samples was isolated using the RNeasy Maxi Kit (Qiagen) and amplified for 1 round using the Ambion MessageAmp aRNA Kit (Ambion Inc.), incorporating amino-allyl UTP into amplified antisense RNA. Sample quality and quantity were assessed by agarose gel electrophoresis, and absorbance was measured at A260 using the Nanodrop 1000 spectrophotometer (Thermo Fisher Scientific). Probes were labeled with Cy3 or Cy5 fluorescent dye and hybridized to Agilent 44K whole human genome expression oligonucleotide microarray slides (Agilent Technologies Inc.), following the manufacturer's suggested protocols. Fluorescence array images were collected for Cy3 and Cy5 using the Agilent DNA microarray scanner G2565BA (Agilent Technologies Inc.), and Agilent Feature Extraction software was used to grid, extract, and normalize data. The data were filtered to exclude Feature Outliers and Population Outliers, as defined by the software, and spots with average signal below 300 were also removed. The Statistical Analysis of Microarray (SAM) program (http://www-stat.stanford.edu/~tibs/SAM/) was used to analyze expression differences between groups. Unpaired, 2-sample *t* tests were calculated for each probe and controlled for multiple testing by estimation of *q* values using the false discovery rate (FDR) method. These results were reduced to unique genes by eliminating all but the highest scoring probe for each gene.

In vivo tumor growth assays. To study the in vivo effect of the AR^{v567es} variant, 3×10^6 LNCaP cells transfected with control pcDNA (LNCaP pc) or AR^{v567es} (LNCaP AR^{v567es}) were injected 1:1 with Matrigel s.c. in the flank of athymic nude-Fox$_n$1^{nu} mice (Harlan Sprague Laboratories). Ten male mice, aged 4–6 weeks, were used in each experimental group. Animals were weighed twice a week. Tumors were measured twice weekly, and tumor volume was estimated by the formula volume = $(l \times w^2)/2$, where l stands for length and w stands for width. Following a University of Washington IACUC-approved animal protocol, some animals were euthanized at specified time points, or when tumors reached a volume of 1,000 mm^3, or when animal weight loss exceeded 20% of initial body weight. After euthanization, tumors were collected. A portion of the tumor was fixed in 10% neutral buffer formalin and embedded in paraffin. Five-micrometer sections were prepared for immunohistochemistry staining. The remaining portions of the tumor were separated into single cells mechanically by mincing and filtering through 70-μm nylon sieves.

To determine whether the ratio of AR^{v567es} to AR^{fl} may predict the tumor response to castration, we selected LuCaP xenografts with "low," "medium," and "high" ratios of AR^{v567es} to AR; these were LuCaP lines 35, 136, and 86.2, respectively. Clinical assessment of the subjects from which LuCaP 35 and 136 primary tumors were obtained suggests that the patients were responsive to androgen ablation, whereas the 86.2 donor was castrate resistant. These lines were placed s.c. into SCID mice, 24 mice per xenograft. Tumor volume was measured twice weekly. Orbital blood was collected biweekly for PSA measurements. When tumor volumes reached 100–200 mm^3, half of the mice were castrated. All mice were followed until tumor volumes began reaching 1,000 mm^3. At this point, all the mice were euthanized in accordance with guidelines from the University of Washington IACUC. At the study end point, tumors were removed and portions were saved for histology, RNA, and protein analysis by Western blot.

Measurements on intratumoral testosterone and DHT. Tissue androgens, including testosterone and DHT, were quantified in xenograft tissues by mass spectrometry, using methods we have published recently (9).

Statistics. All data are displayed as mean ± SEM, except for PCR data in Figure 1, which are displayed as mean ± 1 SD. When 3 or more groups were

compared, 1-way ANOVA was used, followed by Bonferroni-Dunn post-hoc test. (Statview 5.0). When 2 groups were compared, 2-tailed Student's *t* test was used (Excel 2003). A *P* value of 0.05 or less was considered significant. For microarray data, gene expression differences between groups were analyzed with the SAM software by unpaired, 2-sample *t* tests, controlled for multiple testing by estimation of *q* values using the FDR method. Genes identified as significantly altered by *t* test were compared using Venn diagrams, and the functional relevance of those gene sets was determined by GO analysis. The EASE software (http://david.abcc.ncifcrf.gov) was used to calculate overrepresentation statistics for genes in the Venn diagram lists, with respect to all genes represented in the data set. Essentially, for each term within the categories tested (GO biological processes, GO cellular components, GO molecular functions, KEGG pathways, and GenMAPP pathways) the Fisher exact probability of overrepresentation was calculated and used to generate the EASE score by weighting significance of those terms supported by many genes. The EASE score was further controlled for multiple testing, using the FDR with those with a P value of less than 0.05.

Acknowledgments

We would like to thank Jennifer Wu and Marco Marcelli for critical review of the manuscript and Martín Escandón for assistance with manuscript preparation. Grants from the NIH-NCI (PO1 CA 85859 to S.R. Plymate, R. Vessella, and P.S. Nelson), the Pacific Northwest Prostate Cancer SPORE (P50 CA 097186 to S.R. Plymate, R. Vessella, and P.S. Nelson), and the Veterans Affairs Research Program (to S.R. Plymate) supported this work.

Received for publication November 23, 2009, and accepted in revised form June 2, 2010.

Address correspondence to: Stephen R. Plymate, University of Washington School of Medicine, Harborview Medical Center, Box 359625, 325 9th Avenue, Seattle, Washington 98104, USA. Phone: 206.897.5336; Fax: 206.897.5396; E-mail: splymate@u.washington.edu.

1. Scher H, Sawyers C. Biology of progressive, castration-resistant prostate cancer: directed therapies targeting the androgen-receptor signaling axis. *J Clin Oncol*. 2005;23(32):8253–8261.
2. Huggins C, Hodges C. Studies on prostate cancer: effect of castration, estrogen, and androgen injection on serum phosphatases in metastatic carcinoma of the prostate. *Cancer Res*. 1941;1:293–297.
3. Culig Z, et al. Androgen receptor activation in prostatic tumor cell lines by insulin-like growth factor-I, keratinocyte growth factor, and epidermal growth factor. *Cancer Res*. 1994;54(20):5474–5478.
4. Marcelli M, et al. Androgen receptor mutations in prostate cancer. *Cancer Res*. 2000;60(4):944–994.
5. Peterziel H, et al. Mutant androgen receptors in prostatic tumors distinguish between amino-acid-sequence requirements for transactivation and ligand binding. *Int J Cancer*. 1995;63(4):544–550.
6. Tilley W, Buchanan G, Hickey T, Bentel J. Mutations in the androgen receptor are associated with progression of human prostate cancer to androgen independence. *Clin Cancer Res*. 1996;2(2):277–285.
7. Chen C, et al. Molecular determinants of resistance to antiandrogen therapy. *Nat Med*. 2004;10(1):33–39.
8. Montgomery RB, et al. Maintenance of intratumoral androgens in metastatic prostate cancer: a mechanism for castration-resistant tumor growth. *Cancer Res*. 2008;68(11):4447–4454.
9. Mostaghel EA, et al. Intraprostatic androgens and androgen-regulated gene expression persist after testosterone suppression: therapeutic implications for castration-resistant prostate cancer. *Cancer Res*. 2007;67(10):5033–5041.
10. Titus M, Schell M, Lih F, Tomer K, Mohler J. Testosterone and dihydrotestosterone tissue levels in recurrent prostate cancer. *Clin Cancer Res*. 2005; 11(13):4653–4657.
11. Reid AH, Attard G, Barrie E, de Bono JS. CYP17 inhibition as a hormonal strategy for prostate cancer. *Nat Clin Pract Urol*. 2008;5(11):610–620.
12. Steinkamp MP, et al. Treatment-dependent androgen receptor mutations in prostate cancer exploit multiple mechanisms to evade therapy. *Cancer Res*. 2009;69(10):4434–4442.
13. Guo Z, et al. A novel androgen receptor splice variant is up-regulated during prostate cancer progression and promotes androgen depletion-resistant growth. *Cancer Res*. 2009;69(6):2305–2313.
14. Hu R, et al. Ligand-independent androgen receptor variants derived from splicing of cryptic exons signify hormone-refractory prostate cancer. *Cancer Res*. 2009;69(1):16–22.
15. Welsbie DS, et al. Histone deacetylases are required for androgen receptor function in hormone-sensitive and castrate-resistant prostate cancer. *Cancer Res*. 2009;69(3):958–966.
16. Mora G, Mahesh V. Autoregulation of androgen receptor in rat ventral prostate: involvement of c–fos as a negative regulator. *Mol Cell Endocrinol*. 1996; 124(1–2):111–120.
17. Schmudde M, et al. Histone deacetylase inhibitors sensitize tumour cells for cytotoxic effects of natural killer cells. *Cancer Lett*. 2008;272(1):110–121.
18. Sonnemann J, Bumbul B, Beck JF. Synergistic activity of the histone deacetylase inhibitor suberoylanilide hydroxamic acid and the bisphosphonate zoledronic acid against prostate cancer cells in vitro. *Mol Cancer Ther*. 2007;6(11):2976–2984.
19. Angel P, Karin M. The role of Jun, Fos and the AP–1 complex in cell–proliferation and transformation. *Biochim Biophys Acta*. 1991;1072(2-3):129–157.
20. Klampfer L. Signal transducers and activators of transcription (STATs): Novel targets of chemopreventive and chemotherapeutic drugs. *Curr Cancer Drug Targets*. 2006;6(2):107–121.
21. Schreiber M, et al. Control of cell cycle progression by c-Jun is p53 dependent. *Genes Dev*. 1999; 13(5):607–619.
22. Pandini G, et al. Androgens up-regulate the insulin-like growth factor-I receptor in prostate cancer cells. *Cancer Res*. 2005;65(5):1849–1857.
23. Mohler JL, et al. The androgen axis in recurrent prostate cancer. *Clin Cancer Res*. 2004;10(2):440–448.
24. Culig Z, et al. Androgen receptor activation in prostatic tumor cell lines by insulin-like growth factor-I, keratinocyte growth factor and epidermal growth factor. *Eur Urol*. 1995;27(suppl 2):45–47.
25. Goel H, Languino L. Integrin signaling in cancer. *Cancer Treat Res*. 2004;119:15–31.
26. Hobisch A, Culig Z, Radmayr C, Bartsch G, Klocker H, Hittmair A. Androgen Receptor status of lymph node metastases from prostate cancer. *Prostate*. 1996; 28(2):129–135.
27. Putz T, et al. Epidermal growth factor (EGF) receptor blockade inhibits the action of egf, insulin-like growth factor I, and a protein kinase A activator on the mitogen-activated protein kinase pathway in prostate cancer cell lines. *Cancer Res*. 1999; 59(1):227–233.
28. Sadar M. Androgen-independent induction of prostate-specific antigen gene expression via cross-talk between the androgen receptor and protein kinase A signal transduction pathways. *J Biol Chem*. 1999;274(12):7777–7783.
29. Sadar M, Gleave M. Ligand-independent activation of the androgen receptor by the differentiation agent butyrate in human prostate cancer cells. *Cancer Res*. 2000;60(20):5825–5831.
30. Dehm SM, Schmidt LJ, Heemers HV, Vessella RL, Tindall DJ. Splicing of a novel androgen receptor exon generates a constitutively active androgen receptor that mediates prostate cancer therapy resistance. *Cancer Res*. 2008;68(13):5469–5477.
31. Haelens A, Tanner T, Denayer S, Callewaert L, Claessens F. The hinge region regulates DNA binding, nuclear translocation, and transactivation of the androgen receptor. *Cancer Res*. 2007; 67(9):4514–4523.
32. O'Mahony OA, Steinkamp MP, Albertelli MA, Brogley M, Rehman H, Robins DM. Profiling human androgen receptor mutations reveals treatment effects in a mouse model of prostate cancer. *Mol Cancer Res*. 2008;6(11):1691–1701.
33. Centenera MM, Harris JM, Tilley WD, Butler LM. The contribution of different androgen receptor domains to receptor dimerization and signaling. *Mol Endocrinol*. 2008;22(11):2373–2382.
34. Alam TN, et al. Differential expression of CD44 during human prostate epithelial cell differentiation. *J Histochem Cytochem*. 2004;52(8):1083–1090.
35. Knudsen KE, Diehl JA, Haiman CA, Knudsen ES. Cyclin D1: polymorphism, aberrant splicing and cancer risk. *Oncogene*. 2006;25(11):1620–1628.
36. Konrad L, et al. Alternative splicing of TGF-betas and their high-affinity receptors T beta RI, T beta RII and T beta RIII (betaglycan) reveal new variants in human prostatic cells. *BMC Genomics*. 2007;8:318.
37. Krick R, Jakubiczka S, Arnemann J. Expression, alternative splicing and haplotype analysis of transcribed testis specific protein (TSPY) genes. *Gene*. 2003;302(1–2):11–19.
38. Jackson-Cook C, Bae V, Edelman W, Brothman A, Ware J. Cytogenetic characterization of the human prostate cancer cell line P69SV40T and its novel tumorigenic sublines M2182 and M15. *Cancer Genet Cytogenet*. 1996;87(1):14–23.
39. Plymate S, Ware J, Tennant M, Thrasher J, Chatta K, Birnbaum R. The effect on the insulin-like growth factor system in human prostate epithelial cells of immortalization and transformation by simian virus-40 T antigen. *J Clin Endocrinol Metab*. 1996; 81(10):3709–3716.
40. Bae V, Jackson-Cook C, Maygarden S, Chen J, Plymate S, Ware J. Metastatic sublines of an SV40 large T antigen immortalized human prostate epithelial cell line. *Prostate*. 1998;34(4):275–282.
41. Plymate S, et al. Androgen receptor (AR) expression in AR-negative prostate cancer cells results in differential effects of DHT and IGF-I on proliferation and AR activity between localized and metastatic tumors. *Prostate*. 2004;61(3):276–290.
42. Corey E, et al. Establishment and characterization of osseous prostate cancer models: intra-tibial injection of human prostate cancer cells. *Prostate*. 2002; 52(1):20–23.

43. Corey E, et al. LuCaP 35: A new model of prostate cancer progression to androgen independence. *Prostate*. 2003;55(4):239–246.
44. Corey E, Quinn J, Vessella R. A novel method of generating prostate cancer metastases from orthotopic implants. *Prostate*. 2003;56(2):110–114.
45. Wu JD, et al. Combined in vivo effect of A12, a type 1 insulin-like growth factor receptor antibody, and docetaxel against prostate cancer tumors. *Clin Cancer Res*. 2006;12(20 pt 1):6153–6160.
46. Birnbaum R, Ware J, Plymate S. Insulin-like growth factor-binding protein-3 expression and secretion by cultures of human prostate epithelial cells and stromal fibroblasts. *J Endocrinol*. 1994; 141(3):535–540.
47. Roudier MP, et al. Bone histology at autopsy and matched bone scintigraphy findings in patients with hormone refractory prostate cancer: the effect of bisphosphonate therapy on bone scintigraphy results. *Clin Exp Metastasis*. 2003;20(2):171–180.
48. Shariat SF, et al. Comparison of immunohistochemistry with reverse transcription-PCR for the detection of micrometastatic prostate cancer in lymph nodes. *Cancer Res*. 2003;63(15):4662–4670.
49. Page S, et al. Persistent intraprostatic androgen concentrations after medical castration in healthy men. *J Clin Endocrinol Metab*. 2006;91(10):3850–3856.
50. Page ST, et al. Effect of medical castration on CD4+ CD25+ T cells, CD8+ T cell IFN-gamma expression, and NK cells: a physiological role for testosterone and/or its metabolites. *Am J Physiol Endocrinol Metab*. 2006;290(5):E856–E863.
51. Schayek H, Haugk K, Sun S, True LD, Plymate SR, Werner H. Tumor suppressor BRCA1 is expressed in prostate cancer and controls insulin-like growth factor I receptor (IGF-IR) gene transcription in an androgen receptor-dependent manner. *Clin Cancer Res*. 2009;15(5):1558–1565.
52. Wu J, Haugk K, Plymate S. Activation of pro-apoptotic p38–MAPK pathway in the prostate cancer cell line M12 expressing a truncated IGF–IR. *Horm Metab Res*. 2003;35(11–12):751–757.